

Non-destructive testing and evaluation of composite materials/structures: A state-of-the-art review

Bing Wang^{1,2*}, Shuncong Zhong², Tung-Lik Lee³, Kevin S Fancey⁴, Jiawei Mi⁴

¹ Department of Engineering, University of Cambridge, Cambridge CB2 1PZ, UK

² School of Mechanical Engineering and Automation, Fuzhou University, Fuzhou 350116, China

³ ISIS Neutron and Muon Source, Rutherford Appleton Laboratory, Harwell Oxford, Didcot, OX11 0QX, UK

⁴ Department of Engineering, University of Hull, Hull, HU6 7RX, UK

* Corresponding to: bw407@cam.ac.uk (B Wang)

Abstract:

Composite materials/structures are advancing in product efficiency, cost-effectiveness and the development of superior specific properties. There are increasing demands in their applications to load-carrying structures in aerospace, wind turbines, transportation, and medical equipment, *etc.* Thus robust and reliable non-destructive testing (NDT) of composites is essential to reduce safety concerns and maintenance costs. There have been various NDT methods built upon different principles for quality assurance during the whole lifecycle of a composite product. This paper reviews the most established NDT techniques for detection and evaluation of defects/damage evolution in composites. These include acoustic emission, ultrasonic testing, infrared thermography, terahertz testing, shearography, digital image correlation, as well as X-ray and neutron imaging. For each NDT technique, we cover a brief historical background, principles, standard practices, equipment and facilities used for composite research. We also compare and discuss their benefits and limitations, and further summarise their capabilities and applications to composite structures. Each NDT technique has its own potential and rarely achieves a full-scale diagnosis of structural integrity. Future development of NDT techniques for composites will be directed towards intelligent and automated inspection systems with high accuracy and efficient data processing capabilities.

Keywords:

Non-destructive Testing; Composite Materials; Structures; Defects; Damage; Detection & Evaluation; Structural Health Monitoring.



LIST OF CONTENTS

| | | |
|----------|--|-----------|
| 1 | Introduction..... | 1 |
| 2 | Defects and damage evolution in composites | 2 |
| 3 | Non-destructive testing & evaluation techniques | 4 |
| 3.1 | Visual inspection | 7 |
| 3.2 | Acoustic emission | 7 |
| 3.3 | Ultrasonic testing | 9 |
| 3.4 | Infrared thermography | 11 |
| 3.5 | Terahertz testing | 13 |
| 3.6 | Shearography | 15 |
| 3.7 | Digital image correlation | 17 |
| 3.8 | Imaging techniques | 18 |
| 3.8.1 | X-ray imaging | 20 |
| 3.8.2 | Neutron imaging | 22 |
| 4 | Conclusions and outlook | 25 |
| | Funding | 29 |
| | Declaration of conflicting interests..... | 29 |
| | References | 29 |



LIST OF FIGURES

| | | |
|-----------|--|----|
| Figure 1 | Manufacturing-induced flaws/defects, and in-service damage evolution of a composite material/structure, with their potential scale dimensions. | 3 |
| Figure 2 | Categories of non-destructive testing and evaluation techniques. | 4 |
| Figure 3 | Diagram of the electromagnetic spectrum, defining the various regions of radiation according to their range of frequencies and wavelengths. | 5 |
| Figure 4 | A comparison of publication numbers on various NDT methods and their applications to composite materials/structures in the last 30 years; data are retrieved from Web of Science Core Collection database. | 6 |
| Figure 5 | Schematic of localised transient changes in stored elastic energy within a material system under loading, showing the measuring principle of the acoustic emission based NDT technique. | 8 |
| Figure 6 | Principle of ultrasonic testing a composite material in transmission mode. | 10 |
| Figure 7 | Schematic of the measurement principles for an infrared thermography system in reflection mode. | 12 |
| Figure 8 | Schematic showing the measurement principles of THz time-domain spectroscopy using photoconductive antennas. | 14 |
| Figure 9 | Schematic illustration of a shearography system. | 16 |
| Figure 10 | Schematic of a typical stereo-DIC setup for strain mapping of a composite sample sprayed with stochastic speckle pattern. | 17 |
| Figure 11 | Schematic of synchrotron and neutron measurement techniques: (a) diffraction; (b) small-angle scattering; (c) reflectometry; (d) spectroscopy. | 19 |
| Figure 12 | Schematic representation of laboratory-based X-ray imaging. | 20 |
| Figure 13 | Schematic representation of a time-of-flight neutron strain scanner at the ENGIN-X. The elastic strain is measured along the directions of the impulse exchange vectors, q_1 and q_2 , through the two detectors. | 23 |



LIST OF TABLES

| | | |
|----------|---|----|
| Table 1 | Summary of suppliers of devices and systems used for the acoustic emission-based NDT technique; parameters are extracted from literature. | 9 |
| Table 2 | Summary of suppliers for the ultrasonic-based NDT technique; parameters are extracted from published references as practical guidance to their applications to composite research..... | 11 |
| Table 3 | Summary of commercial infrared thermography systems and their key parameters applied to composite research. | 13 |
| Table 4 | Summary of THz-based NDT system suppliers; key parameters are adopted as examples from published research..... | 15 |
| Table 5 | Summary of commercialised shearography system suppliers, and their key parameters applied to composite research. | 16 |
| Table 6 | Summary of suppliers of DIC systems and their key parameters applied to composite research..... | 18 |
| Table 7 | Summary of third and fourth-generation synchrotron light sources in operation and under construction world-wide; brilliance (brightness) is shown in photons/s/mrad ² /mm ² /0.1%bw. | 22 |
| Table 8 | Summary of neutron source facilities world-wide and their basic parameters.. | 24 |
| Table 9 | Benefits and limitations of established non-destructive testing techniques used in composite research..... | 25 |
| Table 10 | Applications and capabilities of established NDT techniques for composite inspection and evaluation..... | 27 |



1 Introduction

Composite materials/structures are advancing in product efficiency, cost effectiveness, and the development of superior specific properties (strength and modulus). There are increasing demands in their applications to load-bearing structures in aerospace, wind turbines, transportation, and medical equipment *etc.* [1]. Manufacturing of composite materials is a multivariable task, involving many procedures, where various types of defects may occur within a composite product, giving rise to significant safety concerns in service [2]. Detection and evaluation to maintain structural integrity are particularly challenging since composites are usually non-homogeneous and anisotropic. Defects and damage can occur within numerous locations at various levels of scale, making it difficult to track all the damage sites which can result in complex damage mechanisms [3]. In addition, damage accumulation within a composite is closely related to the actual strength, stiffness and lifetime prediction of the component. Therefore, robust and reliable non-destructive testing (NDT) of composites is essential for reducing safety concerns, as well as maintenance costs [4] to minimise possibilities for process disruption and downtime. These factors attract interest both from academic researchers and industrial engineers.

There are a wide variety of NDT techniques built upon different principles. These have demonstrated effectiveness in quality assurance throughout the whole lifecycle of composite products; *i.e.* in process design and optimisation, process control, manufacture inspection, in-service detection, and structural health monitoring [5]. There are reviews available on NDT methods used for composites research over different timelines, focusing on various aspects: for general methods and trends over last 30 years refer to [4,6–11]; specific areas include those which concentrate on porosity in composite repairs [12], crack damage detection [13], bond defect determination in laminates [14], thick-wall composites [15], sandwich structures [16,17], large-scale composites [18], smart structures [19], as well as inspection and structural health monitoring of composites [20,21], especially for marine [22], wind turbine [23–26], and aerospace applications [27,28]. Audiences are recommended to refer to further information on their specific interests.



This paper reviews the most established NDT techniques for detection and evaluation to ensure the structural integrity of composite materials/structures; however, a full description of all methods is beyond the scope of this paper. Instead, we aim to provide a practical review of the established and emerging NDT techniques and their applications to composite research. The American Society for Testing and Materials (ASTM) has developed more than 130 standards, guides, and practices, containing technical specifications, criteria, requirements, procedures and practices for most of the NDT techniques [29]. We also include the standard practices for each NDT method available from the ASTM to provide guidance for researchers and engineers. These make it a unique state-of-the-art review paper to cover the most up-to-date practical information for NDT techniques and their applications to composite materials and associated structures.

The paper is organised as follows. Section 2 introduces the potential defects and damage evolution in composites. Section 3 provides an overview of development and principles of NDT techniques, and then elaborates on eight well-established NDT methods in subsections, covering a brief historic background, principles, standard practices, equipment and facilities for each NDT method in composite research. These include visual inspection (Section 3.1), acoustic emission (Section 3.2), ultrasonic testing (Section 3.3), infrared thermography (Section 3.4), terahertz testing (Section 3.5), shearography (Section 3.6), digital image correlation (Section 3.7), as well as X-ray and neutron imaging (Section 3.8). Section 4 compares and discusses the benefits and limitations of above NDT techniques, and further summarises their capabilities and applications to composite structures. This paper is concluded by the further development of NDT techniques, which is driven by intelligent and automated inspection systems with high accuracy and efficiency in data processing.

2 Defects and damage evolution in composites

Manufacturing-induced flaws/defects can occur in many forms: unevenly distributed fibres cause resin-rich regions; laminate-tool interactions result in in-plane fibre waviness or out-of-plane fibre wrinkling [30,31]; voids and porosities arise from poor resin infusion; inclusions from contaminated ambient conditions; misalignment of ply and fibre orientation; matrix cracking, laminate warping and buckling from build-up of thermal residual stresses during curing *etc.* [32,33]. Flaws/defects act as stress concentration points, promoting crack



propagation and delamination to reduce effective strength, stiffness and service time of composite products [34]. Although residual stresses can occasionally be beneficial, especially for producing morphing composite structures [35–38], they are usually detrimental [32]. A wide range of processes have developed for the moulding of composite materials to reduce flaws, defects and build-up residual stresses that may occur during manufacture. These can involve multi-step processing, expensive consumables and equipment, to meet technical requirements. Typical industrial practice generally includes NDT inspection and evaluation of composite products to ensure their structural integrity and mechanical performance, which can be particularly challenging [39].

Figure 1 summarises the typical flaws and defects that may occur during manufacturing, and the in-service damage evolution of a composite material/structure. There are no clear boundaries on the scales of different defects and damage (which also depend on composite constituents); thus here we provide a general guidance according to the published literature.

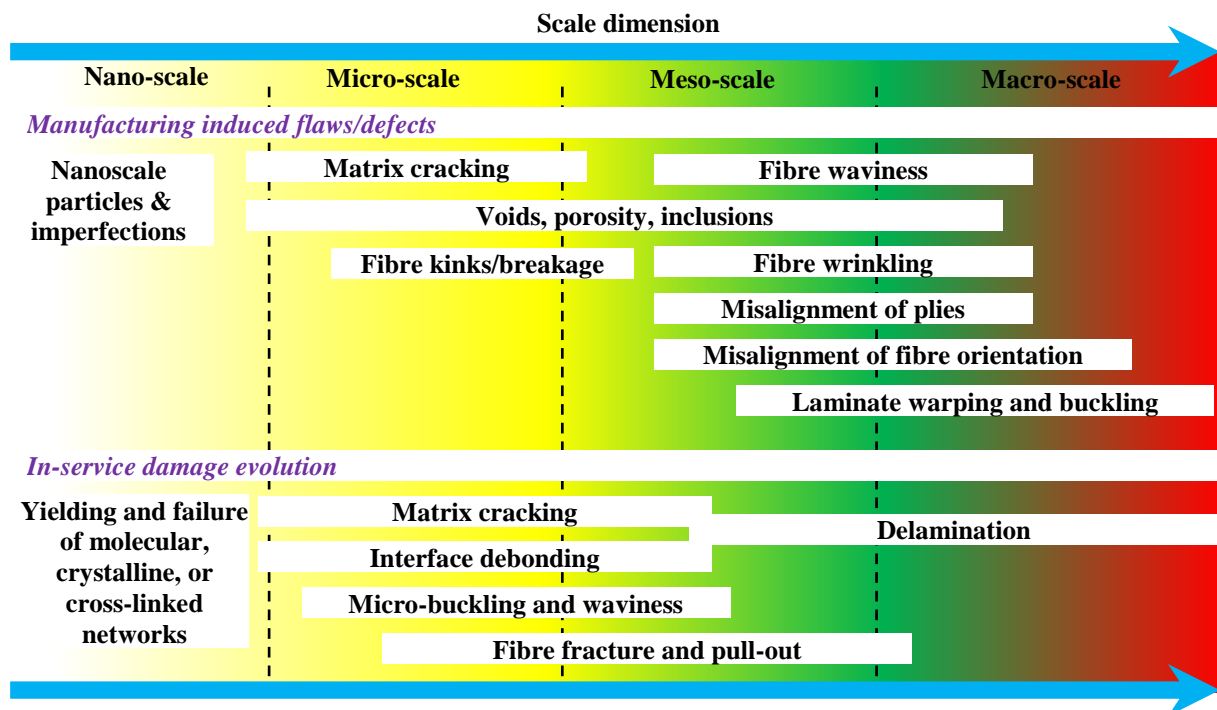


Figure 1 Manufacturing-induced flaws/defects, and in-service damage evolution of a composite material/structure, with their potential scale dimensions.

In-service damage evolution within a composite material/structure depends on composite constituents and loading conditions. Their failure processes are an accumulation of basic

rupture mechanisms that include matrix cracking, fibre/matrix debonding, fibre fracture and pull-out, micro-buckling and waviness, delamination, *etc.* [40,41]. The damage process initiates at the nano- or micro-scale, where molecular chains, crystals and amorphous regions (for semi-crystalline thermoplastic polymers) or cross-linked molecular networks (for thermosetting polymers) carry loads until their limits are reached; damage then starts to accumulate on the micro-scale through crack propagation, interface debonding and micro-buckling, fibre fracture and pull-out, which lead to delamination, ultimately developing into macro-scale failure.

3 Non-destructive testing & evaluation techniques

The term ‘non-destructive testing’ covers a wide range of analytical techniques to inspect, test or evaluate chemical/physical properties of a material, component or system without causing damage. Early established NDT techniques include ultrasonic, X-ray radiography, liquid penetrant testing, magnetic-particle testing and eddy-current testing, which were initially developed for steel industry. Among these, ultrasonic and radiographic detection are also effective inspection techniques for composite structures [17]. It is difficult to select appropriate NDT techniques for a specific purpose; however, ASTM E2533 [5] serves as a practical guide in using NDT methods on composite materials/structures for aerospace applications.

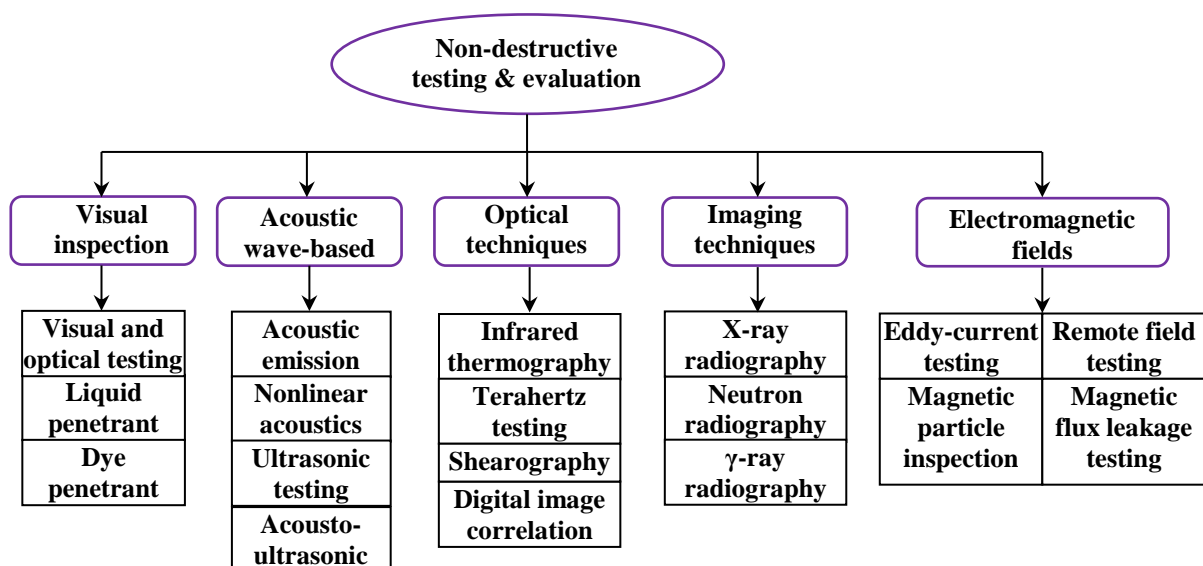


Figure 2 Categories of non-destructive testing and evaluation techniques.



To date, there have been numerous NDT methods based on different principles, see Figure 2. They can be categorised into five groups: (i) visual inspection (i.e. those visible to the human eye); (ii) acoustic wave-based techniques, such as acoustic emission, nonlinear acoustics, and ultrasonic waves; (iii) optical techniques, which include infrared thermography, terahertz testing, shearography, digital image correlation; (iv) imaging-based techniques, e.g. X-ray/neutron radiography/tomography and micro-tomography [4]; (v) electromagnetic field based techniques, such as eddy-current testing, remote field testing, magnetic-particle inspection and magnetic flux leakage testing [42].

Here, we focus on eight established and emerging NDT techniques and their applications to composite research in categories (i) to (iv), with the exclusion of category (v). Since NDT methods in (v) are based on electromagnetic induction, their applications are limited to conductive materials [43]. Eddy-current testing (ECT) for example, is well-established and widely used for detecting cracks and corrosion in homogeneous metallic materials. Although it may be applicable to carbon composites, their conductivities are usually very low and inhomogeneous due to the lay-up and bundling of the conductive fibres [44]. This leads to further issues and difficulties for ECT to be an efficient and cost-effective solution for most composite NDT applications.

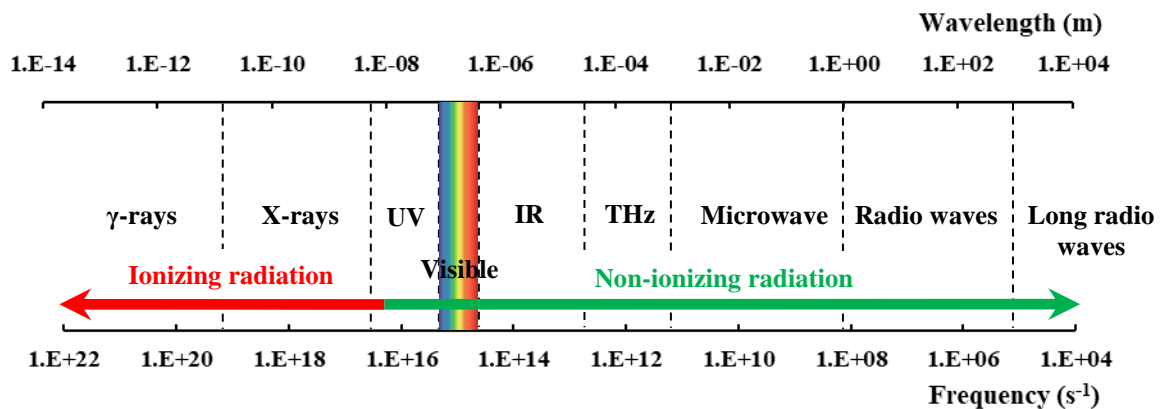


Figure 3 Diagram of the electromagnetic spectrum, defining the various regions of radiation according to their range of frequencies and wavelengths.

The measurement principles of each elaborated NDT technique depend on the characteristics of the electromagnetic waves based. Figure 3 shows the electromagnetic spectrum with divided wavelength sub-regions: the soft boundaries indicate terminologies for the subsections. Developments in generation and detection within each spectral regime have

induced numerous industrial applications [45]. Ionizing radiation consists of short-wave ultraviolet (UV), X-rays, gamma-rays or highly energetic particles, such as α -particles, β -particles or neutrons, which are harmful to biological tissues; whereas the remaining part of the spectrum is considered to be non-ionizing radiation.

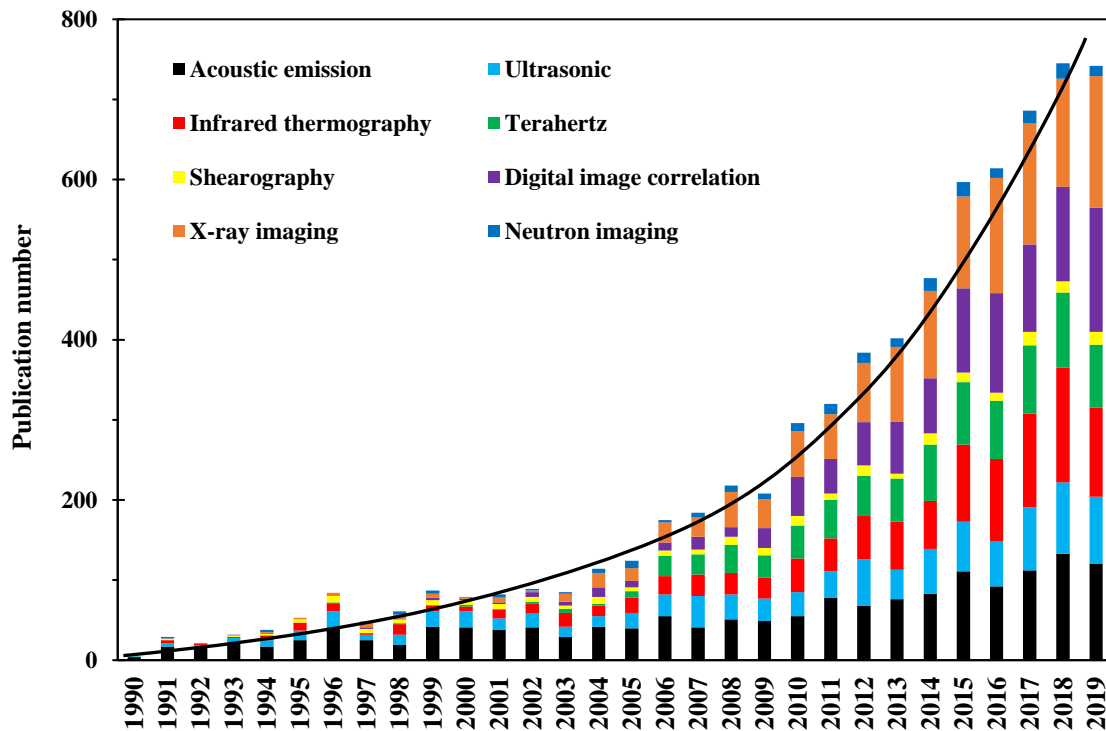


Figure 4 A comparison of publication numbers on various NDT methods and their applications to composite materials/structures in the last 30 years; data are retrieved from Web of Science Core Collection database.

To date, there have been a growing number of research activities in this field. We performed an electronic data-base search on articles published in last 30 years (until 31/12/2019) using the Web of Science Core Collection database, to trace the trends in using various NDT techniques within composite research, see Figure 4. The use of acoustic emission on composites has a long history and is well-established; it is still active in a relatively steady state. Owing to significant developments in equipment manufacture, computing power, imaging processing and acquisition techniques over last three decades, there have been rapid increases in the application of infrared thermography, ultrasonic, digital image correlation and X-ray imaging to non-destructive detection and evaluation of composite materials/structures. Terahertz (THz)-based NDT technology has become a promising technique for composite inspection within last decade [46,47]. Research papers on the shearography technique is low,

but it was promoted significantly by the invention of the laser in the 1960s [48], thus it is well-established and widely used for industrial NDT, especially in aerospace [49,50]. Although neutron imaging shares similar principles to X-ray imaging, the generation of neutrons is more expensive than for X-rays, the former requiring either a nuclear reactor or spallation process [51]. This has resulted in relatively few publications on its application to composite materials.

3.1 Visual inspection

Visual inspection (VI) is the most basic type of NDT technique to inspect damage. It is quick, economically viable, and flexible, while its disadvantages are quite obvious and significant [11]. VI methods include visual & optical testing (VOT) and penetrant testing (PT). VOT analysis is a leading procedure in the monitoring of surface imperfections for acceptance-rejection criteria during composite parts production [52]. The PT technique is a widely applied, low-cost inspection method. It has been used in non-porous materials to detect casting, forging, and welding surface defects including cracks, surface porosity, leaks in new products, and in-service fatigue cracks *etc.*

VI methods are particularly effective in detecting macroscopic flaws, such as poor joints, erroneous dimensions, poor surface finish and poor fits. It usually employs easy-to-handle equipment such as miniature cameras or endoscopes [23]. VI studies of small integrated circuits have shown that the modal duration of eye fixation from trained inspectors was ~200 ms. Here, variation by a factor of six in inspection speed led to a variation of less than a factor of two in inspection accuracy; inspection accuracy also depends on training, inspection procedures, and apparatus (optics, lighting, *etc.*) [53].

3.2 Acoustic emission

Damage occurrences within a composite produce localised transient changes in stored elastic energy; the energy releases stress waves, resulting in fibre breakage, matrix cracking, debonding, delamination *etc.* [3]. Acoustic emission (AE) based NDT techniques detect and track these sudden releases of stress waves through arrays of highly sensitive sensors or transducers [54], as illustrated in Figure 5. Use of the AE method started in the early 1950s, when Kaiser first used electronic instrumentation to detect audible sounds produced by tensile



deformation of a metallic specimen [55]. His discovery on the effect of sample stress history on the production of AE became known as the ‘Kaiser effect’ [56]. AE was first applied to the study of composite materials in the 1970s [3], and it has now been widely used in various aspects of composite research [57].

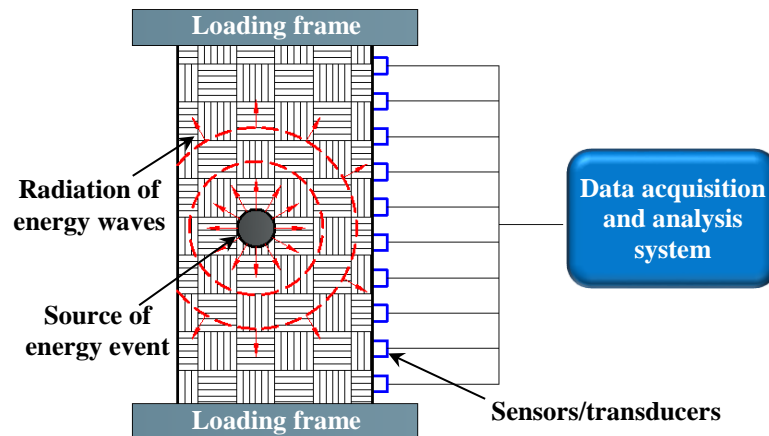


Figure 5 Schematic of localised transient changes in stored elastic energy within a material system under loading, showing the measuring principle of the acoustic emission based NDT technique.

The AE method is unique in that: (i) the signals, i.e. stress waves, are emitted by the testing sample, not from external sources (as with other NDT methods); (ii) strain or displacement data are usually recorded, rather than as geometrical defects; (iii) it monitors dynamic processes in a material, tracking the development of certain defects, which significantly benefits fatigue tests. It has been reported that AE-based NDT can detect fatigue cracks, fibre fractures, matrix micro-cracks, interface debonding, as well as delamination [11]. However, there are also certain difficulties. Data collected during the loading of a composite system can be in different forms, the most common is the AE amplitude signal. Processing and analysis of data are time-consuming and require certain skills and experience [3]: in particular, the distribution of amplitudes exhibit overlapped areas, which sometimes causes difficulties in associating these with the damage mechanisms.

Efforts have been made to address these issues. A common approach is to analyse multiple parameters to complement the damage analysis, such as cumulated event counts [58,59], energy [60], duration [61], or frequency of the received amplitude signals [62]. Other solutions include verifying damage modes through other methods, for example, microscopy, to provide more reliable analysis [63]. Table 1 summarises some of the commercial suppliers

of AE-based NDT systems, which may be applied to composite research. Standardised practices of using AE include: ASTM E1067 on examining GFRP tanks/vessels [64]; ASTM E1118 on composite pipes [65]; ASTM E2191 on filament-wound composite pressure vessels [66]; ASTM E2076 on composite fan blades [67]; as well as ASTM E2661 on plate-like and flat composite structures for aerospace [68].

Table 1 Summary of suppliers of devices and systems used for the acoustic emission-based NDT technique; parameters are extracted from literature.

| Supplier | Resolution (bit) | Dynamic range (dB) | Bandwidth (MHz) | Sampling speed (MHz) | Ref |
|-----------------------------|------------------|--------------------|-----------------|----------------------|---------|
| Physical Acoustics Co. | 16 | 100 | 0.001-1.2 | 5-20 | [69–71] |
| Meggitt Endevco | -- | 100 | 0.002-1.0 | -- | [63] |
| Soundwel Technology Co. Ltd | 16 | 85 | 0.001-2.5 | 0.5-10 | [72] |
| IPPT PAN | -- | 40 | 0.005-0.5 | -- | [73] |
| Vallen Systeme | -- | 100 | 0.1-0.45 | -- | [74] |

*Please note the information in this table is incomplete, and not for advertising purposes – it should not be taken as endorsements by the authors.

There is also some interest in a combined method of acoustic emission and ultrasonic testing, namely the acousto-ultrasonic technique (AUT), as first introduced by Vary in 1981 [75]. By adopting the ultrasonic transducer, repeated ultrasonic pulses are introduced into a material, resultant waveforms carry the morphological information that contribute to damage mechanisms. A concept of ‘stress wave factor’ is defined as a relative measurement of efficiency of energy dissipation to indicate regions of damage [76]. In NDT, the AUT is mainly used to determine the severity of internal imperfections and inhomogeneities in composites [11].

3.3 Ultrasonic testing

Ultrasonic testing (UT) is an acoustic inspection technique, which is expanding rapidly into many areas of manufacturing and in-service detection [77]. It operates through surface wave testing, bulk wave propagation and guided wave propagation, while the guided wave analysis technique is superior for anisotropic materials [78]. For further information, the use of ultrasonic bulk wave testing in sizing of flaws has been reviewed by Felice and Fan [79].



For NDT inspection of composite materials, elastic waves or ‘Lamb waves’ propagate in selective directions owing to their anisotropic nature which makes the technique effective. UT operates in three detection modes, i.e. reflection, transmission and back-scattering of pulsed elastic waves in a material system [17]. It introduces guided high frequency sound waves (ranging from 1 KHz to 30 MHz [4]) to effectively detect flaw size, crack location, delamination location [80], fibre waviness [31], meso-scale ply fibre orientation [81], and layup stacking sequence [82].

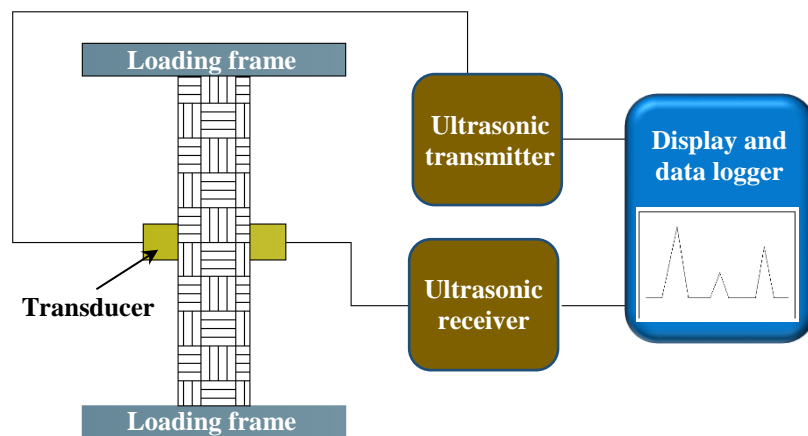


Figure 6 Principle of ultrasonic testing a composite material in transmission mode.

There are various types of UT systems with hundreds of guided wave modes and frequencies being available [78]. A typical UT system consists of a transmitter and receiver circuit, transducer tool, and display devices, see Figure 6. The transmitter can either be arranged at an angle to the sample, or in the form of phased array [83]. The guided Lamb waves can be generated by means of (i) ultrasonic probe, (ii) laser, (iii) piezoelectric element, (iv) interdigital transducer, or (v) optical fibre [84].

The potential types of damage that guided Lamb wave-based NDT can provide are summarised by Rose [77]; the mode selection, generation and collection, modelling and simulation, signal processing and interpretation have been well-documented by Su *et al.* [84]. A later review on guided waves for damage identification in pipeline structures is provided by Guan [85]. Table 2 provides some suppliers of UT equipment which may be applied to composites research. UT techniques for composites have been standardised: ASTM E2373 gives the requirements for developing a time-of-flight UT examination [86]; ASTM E2580 for

inspections on flat composite panels and sandwich structures in aerospace applications [87]; ASTM E2981 for filament wound pressure vessels in aerospace applications [88].

Table 2 Summary of suppliers for the ultrasonic-based NDT technique; parameters are extracted from published references as practical guidance to their applications to composite research.

| Supplier | Resolution (bit) | Dynamic range (dB) | Bandwidth (MHz) | Sampling speed (MHz) | Ref |
|------------------------------|------------------|--------------------|-----------------|----------------------|------|
| ZETEC Inc. | 16 | -- | 0.5-18 | 50 or 60 | [89] |
| Inspection Technology Europe | 16 | 90 | 0.1-30 | 50/160 | [90] |
| Advanced Technology Group | 12 | 80 | 1-22 | 100 | [91] |
| Peak NDT | 16 | 60 | 0.001-40 | 10-100 | [92] |
| Olympus | -- | 60 | 0.2-20 | -- | [93] |
| Polytec Co. | 14 | | 0-25 | | [94] |

*Please note the information in this table is incomplete, and not for advertising purposes – it should not be taken as endorsements by the authors.

3.4 Infrared thermography

Infrared thermography (IRT) is a method used to detect and process infrared energy emissions from an object by measuring and mapping thermal distributions [95]. Infrared energy is electromagnetic radiation with wavelengths longer than visible light, see Figure 3. The discovery of thermal radiation dated back to the early 1800s [52]. Every object with a temperature higher than absolute zero emits electromagnetic radiation that falls into the infrared spectrum [96]. IRT has undergone rapid development in the last 30 years with developments in infrared cameras, data acquisition and processing techniques. It provides capabilities in terms of non-contact, non-invasive, real-time measurement, high resolution, and covering large volumes [97].

The IRT method is effectively used to monitor the entire life of a product, from manufacturing (on-line process control), to the finished product (NDT evaluation) and to in-service maintenance and diagnostics [52]. It has been applied to research and various aspects within industry, including non-destructive testing [98], building diagnostics [99], adhesion science [52], condition monitoring [100], predictive or preventive maintenance [101], medical diagnostics [102], veterinary medicine [103], and many more. As for composite materials and structures, IRT-based NDT has also been widely used, especially during manufacturing for



aerospace applications. It is used to detect inclusions, debonding, delamination, and cracked networks [27]. Both Boeing and Airbus have used IRT for structural health monitoring to ensure the integrity of their composite products [97].

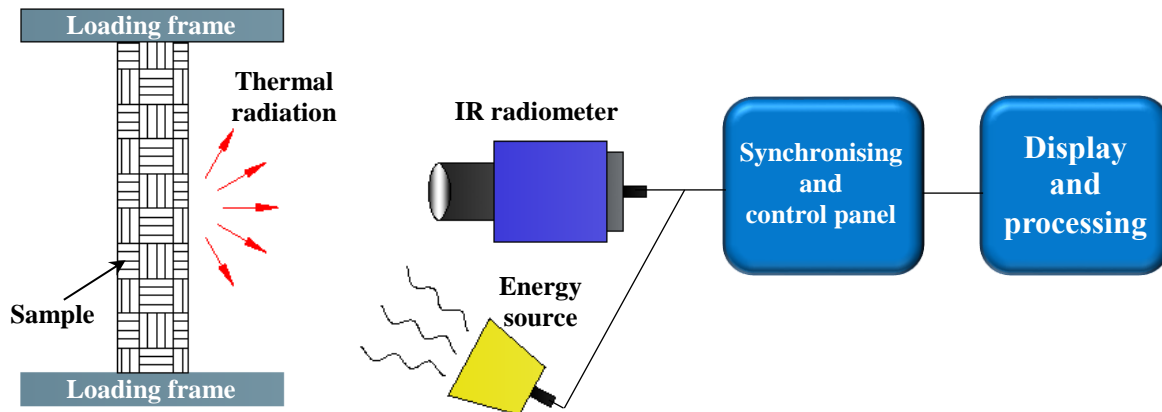


Figure 7 Schematic of the measurement principles for an infrared thermography system in reflection mode.

A typical IRT system contains an infrared radiometer, with/without energy source, synchronising and control panel, display software, see Figure 7. The radiometer is the core of the IRT system, it absorbs IR energy emissions and converts them into electrical voltage or current signals. They are then transmitted and displayed as infrared images of temperature distribution [52]. The use of IRT can be implemented through (i) passive and (ii) active thermography [104]. In passive thermography (PT), thermal radiation is directly emitted from surfaces of the test body under natural conditions and subsequently monitored. For active thermography (AT), a heating or cooling flow is generated and propagated into the test object, thermal responses according to the Stefan-Boltzmann law are then detected and recorded to reveal internal structures. Recent advances in signal processing techniques and equipment developments have made the AT method more practical and effective than the conventional PT approach [105,106].

Based on energy stimulation methods, the AT method has developed into different categories. First, optical thermography is the most traditional form of IRT, using optical sources such as photographic flashes, halogen lamps, or lasers, which are also known as pulsed thermography (PT) [107], modulated (lock-in) thermography (MT) [108], or laser thermography (LT) [109,110], respectively. Second, induction thermography, which shares

similar principles to eddy current testing, that uses electronic or magnetic currents to induce energy waves [111–114]. Third, mechanical thermography, which uses mechanical waves to interact with internal structures to detect thermal waves from defects [115]; it can be implemented through vibrothermography [116,117], microwave thermography [118,119], or ultrasonic lock-in thermography (ULT) [120] which attracts increasing interest. Yang and He [121] have presented a comprehensive review of the optical and non-optical IRT methods and their NDT applications in composite materials/structures. Table 3 gives some suppliers of IRT equipment which may be applied to composites research. The reader is referred to ASTM E2582 for standard practice on using IRT with composite panels and repair patches in aerospace applications [122].

Table 3 Summary of commercial infrared thermography systems and their key parameters applied to composite research.

| Supplier | Spatial resolution (mRad) | Thermal sensitivity (mK) | Imaging resolution (pixel ²) | Imaging rate (fps) | Ref |
|---------------------------|---------------------------|--------------------------|--|--------------------|-----------|
| Thermal Wave Imaging Inc. | 1.13 | 25 | 320×256 | 60 | [123,124] |
| Thermoteknix System Ltd. | 0.47 | 70 | 384×288 | 50 or 60 | [125] |
| Fluke Corporation | 0.93 | 50 | 640×480 | 9 or 60 | [126] |
| InfraTec GmbH | 0.08-1.3 | 20 | 640×512 | 1-100 | [127] |
| Mikron Infrared | 1.0 | 80 | 320×240 | 9 or 50 | [128] |
| Optris | -- | 130 | 382×288 | 80 | [129] |
| NEC Avio | 0.87 | 50 | 320×240 | 60 | [130] |
| FLIR System | 0.19-1.36 | 20 | 320×256 | 50 | [131,132] |

*Please note the information in this table is incomplete, and not for advertising purposes – it should not be taken as endorsements by the authors.

3.5 Terahertz testing

Terahertz (THz) waves lie within the electromagnetic spectrum from 100 GHz to 30 THz [133], which belong to non-ionising radiation and are not harmful to biological tissues (Figure 3). There are many THz wave sources in nature, though previously it has been difficult to generate and detect THz waves, so for many years, there have been few applications [134]. Owing to breakthroughs in ultrafast lasers and ultra-micro machining technologies during the 1980s [135,136], there has been a rapid expansion in applications for THz science and technology [46]. THz-based NDT technology has also started to be a promising technique for



composite inspections [2,47], offering advantages in terms of higher resolution and better penetration in most materials compared to other techniques [137].

THz waves have good penetrating power for non-metallic, non-polar materials, including foams, ceramics, glass, resin, paint, rubber and composites. THz-based NDT techniques use the wave characteristics to detect, analyse and evaluate material systems, which has attracted wide interest in various fields, leading to rapid expansion [138]. Figure 8 shows an example of a typical setup of the THz-based NDT method, presenting the basic measuring principles in transmission mode [45]. The system induces THz short waves into a material, which interact with different phases, inclusions, defects or damage. Internal structures within the material are determined by detection and analysis of reflected or transmitted THz waves. Therefore, the multi-phase and multi-layered nature of composites are well-suited to THz-based NDT – it offers multi-scale, more comprehensive information to detect and reveal internal structures and damage within a composite [47].

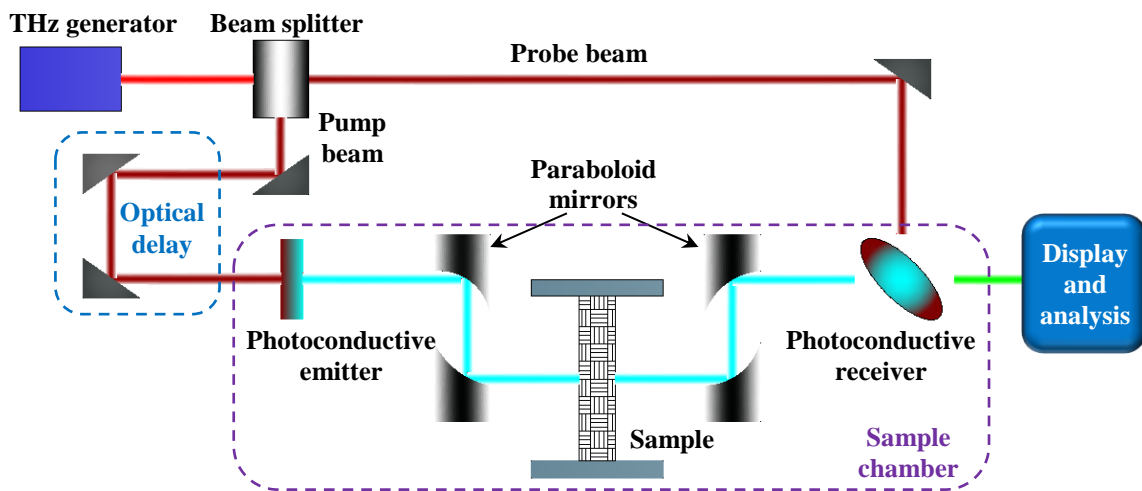


Figure 8 Schematic showing the measurement principles of THz time-domain spectroscopy using photoconductive antennas.

The THz-based NDT technique is usually implemented through (i) a THz time-domain spectroscopy system (THz-TDS), also known as pulsed spectroscopy, or (ii) a continuous wave (THz-CW) system. The detection setup determines how information is evaluated within composite materials. In the THz-TDS system, short pulsed THz waves are generated by optical excitation of a photo-conductive antenna using a laser pulse emitting in the femtosecond regime [133], the time-dependent evolution of the THz electric field of a single pulse is measured,

which can be used to determine phase information within a composite. For the THz-CW system, high power THz waves are produced through gas lasers, quantum cascade lasers or parametric sources [2], and phase information is measured by recording the average intensity (related to the amplitude of the wave) of the electromagnetic field.

Table 4 Summary of THz-based NDT system suppliers; key parameters are adopted as examples from published research.

| THz supplier | Setup | Resolution (bit) | Dynamic range (dB) | Scanning range (mm ²) | Spectrum band (THz) | Ref |
|----------------------|---------|------------------|--------------------|-----------------------------------|---------------------|-----------|
| Virginia Diodes Inc. | THz-CW | -- | 110 | 100×100 | 0.05-1.0 | [137] |
| Zomega Terahertz Co. | THz-TDS | -- | 70 | 150×150 | 0.1-4.0 | [139,140] |
| TeraView | THz-TDS | 16 | 95 | 150×150 | 0.06-3.0 | [141] |
| TeraSense | THz-CW | 16 | -- | 128×64 | 0.05-1.0 | [142] |
| MenloSystems | THz-TDS | 18 | 90 | 150×150 | 0.1-4.0 | [143] |
| Toptica Photonics | THz-CW | -- | 100 | 100×100 | 0.1-6.0 | [144] |
| Luna Ltd. | THz-TDS | 16 | 95 | -- | 0.1-2.0 | [145–147] |

*Please note the information in this table is incomplete, and not for advertising purposes – it should not be taken as endorsements by the authors.

There have been several reviews regarding applications of the THz-based technique, focusing on different aspects: Dhillon *et al.* [46] presented a comprehensive review on the roadmap of THz science and technology; Jansen *et al.* [148] reviewed progress and applications of THz systems in the polymer industry; Amenabar *et al.* [2] summarised the detection and imaging methods using THz waves, as well as their applications in composites; Zhong [47] further summed up the most recent advances. Table 4 shows some of the commercialised THz-based NDT systems and their key parameters. As an emerging NDT technique, standardised practice on using the THz approach is still developing.

3.6 Shearography

Shearography testing (ST) is a laser-based non-contact NDT technique, using a full-field speckle shearing interferometric method to overcome the limitations of holography testing [49]. This technique was first described and applied by Leendertz in the 1970s [149,150]. To date, it has been used in various fields as a practical quantitative inspection tool to detect flaws and defects [151–153], leakage [154], delamination and damage [155,156], as well as measurement of displacement and strain [157,158], curvature [159–162], residual stress [163–



165], mechanical analysis [166,167], surface profiling [168], and dynamic vibration [169–171].

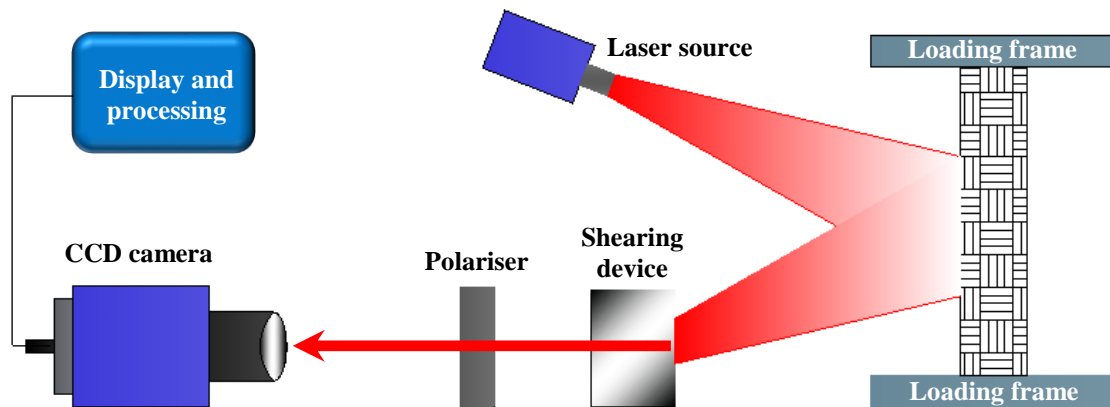


Figure 9 Schematic illustration of a shearography system.

Table 5 Summary of commercialised shearography system suppliers, and their key parameters applied to composite research.

| Supplier | Hardware & software | Inspection area (m ²) | Imaging resolution (pixel ²) | Imaging rate (Hz) | Ref |
|--------------------------------|---------------------|-----------------------------------|--|-------------------|-----------|
| Dantec Dynamics | Yes | 0.01 – 2 | 1392×1040 | 10 | [91,172] |
| ZEISS Optotechnik | Yes | -- | 220×160 | -- | [173] |
| Optonor AS | Yes | 0.01 – 4 | 1936×1216 | -- | [174,175] |
| ISI-sys | Yes | -- | 2560×1920 | -- | [176,177] |
| Laser Optical Engineering Ltd. | Yes | 0.49 | 1280×1024 | 12 | [178] |
| Laser Technology Inc. | Yes | 0.01-0.05 | 1628×1236 | 30 | [179] |

*Please note the information in this table is incomplete, and not for advertising purposes – it should not be taken as endorsements by the authors.

A typical shearography setup is shown in Figure 9. A laser beam illuminates a sample surface, and the beam is then scattered and reflected. The resulting speckle pattern is imaged through a shearing device (Michelson interferometer or diffractive optical element), which divides it into two coherent images with one being monitored during deformation. A controlled stressing process is essential and is applied through thermal [180,181], vacuum [163,182], vibration [153], microwave [183], or mechanical loading [184]. The interferometric pattern is then captured and recorded by a charge-coupled device (CCD camera) which results in a fringe pattern that contains structural information [178]. It has been adopted for inspection and evaluation in various composite products, for example pipes [185,186], sandwich structures [16,17,187], wind turbine blades [188], aerospace structures [189–191], as well as racing tyres

[192]. Some suppliers of commercialised shearography systems are given in Table 5. An example of standard practice using shearography for polymer composites and sandwich core materials in aerospace is represented by ASTM E2581 [187].

3.7 Digital image correlation

Digital image correlation (DIC) is a simple and cost effective optical NDT technique for measuring strain and displacement, which are critical parameters within engineering and construction projects. It was developed in the 1980s [193], and has become widely used only in recent years due to the rapid development of computers and image acquisition methods. Images are usually captured through CCD cameras, possibly with the aid of microscopy. The DIC system tracks blocks of random pixels on a sample surface, and compares digital photographs at different stages of deformation to build up full field 2D or 3D deformation vector fields and strain maps [194]. Thus, any changes in the structure or surface can easily be reflected to give details on surface strain, deformation, or crack propagation, making it ideal for studies of crack propagation and deformation. It offers more accurate strain monitoring than conventional extensometers or strain-gauges, which often suffer from imperfect attachment to the measured surface and the limitations imposed by values that are averaged over the gauge length [195].

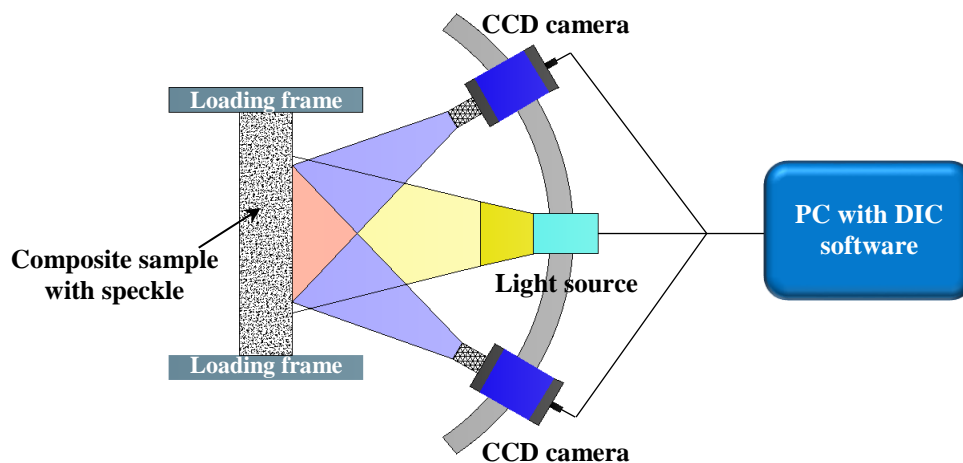


Figure 10 Schematic of a typical stereo-DIC setup for strain mapping of a composite sample sprayed with stochastic speckle pattern.

Figure 10 shows a typical DIC system for strain mapping of a composite sample; here, special illumination may be required. The sample is sprayed with a white stochastic speckle

pattern prior to testing and two CCD cameras need to be calibrated each time. Imaging data can be analysed through commercialised software to reveal changes in speckle with reference images and strain or deformation can be calculated during the tests. Thus, quality of the speckle pattern is vital for accuracy and precision in the DIC technique [196]. Pan [197] presented the historic developments, recent advances and future of DIC for surface deformation measurement; Hild *et al* [198] discussed the capabilities of DIC in damage measurements; Aparna *et al* [199] summarised studies on fatigue testing of composites using the DIC technique. Therefore, they are not elaborated here.

Table 6 summarises some suppliers of DIC systems and certain examples in the literature. Audiences are recommended to refer to each supplier for full details. Given the flexibility and versatility of DIC systems, standardisation of the DIC technique is difficult or even impossible to be applicable to each individual situation [197].

Table 6 Summary of suppliers of DIC systems and their key parameters applied to composite research.

| DIC supplier | Hardware/ Software | Maximum imaging rate (fps) | Imaging resolution (pixel ²) | Precision ($\mu\text{m}/\text{pixel}$) | Strain mapping | Ref |
|----------------------|-----------------------|-------------------------------|---|---|-------------------|-----------|
| Correlated Solutions | Yes/Yes | 5,000,000 | 2240×1680 | -- | 2D & 3D | [200] |
| Limes | Yes/Yes | 2,000,000 | 4096×3068 | 1.0 | 2D & 3D | [201] |
| Dantec Dynamics | Yes/Yes | 1,000,000 | 2560×1920 | 5.0 | 2D & 3D | [202] |
| GOM | Yes/Yes | 2000 | 4096×3068 | 4.8 | 2D & 3D | [203–205] |
| LaVision | Yes/Yes | 150 | 2240×1680 | 5.86 | 2D & 3D | [206] |
| Instron | Yes/Yes | 50 | 1280×720 | 1.0 | 2D | [207] |
| MatchID | No/Yes | -- | -- | -- | 2D & 3D | [208] |
| ISI-sys GmbH | Yes/No | 100 | 1920*1200 | 2.0 | 2D & 3D | [209] |

*Please note the information in this table is incomplete, and not for advertising purposes – it should not be taken as endorsements by the authors.

3.8 Imaging techniques

Imaging techniques refer to the NDT methods that are based on phase contrast imaging, which were first developed in the 1930s [210]. They enable high-resolution imaging (a few angstroms), making it possible to distinguish features at atomic or molecular levels. Developments in digital imaging technology and synchrotron radiation facilities have promoted the use of imaging techniques since the 1990s [211]. To date, it has been reported that X-ray imaging is carried out either through lab-based X-ray tubes or synchrotron light



sources; alternatively, neutron imaging uses neutrons generated from fission reactors or spallation sources [212]. Both X-ray and neutron radiography have developed to be indispensable tools in various research fields ranging from solid matter to soft tissues [211].

Synchrotron X-ray and neutron radiation are NDT techniques that provide insights into micro-structures, residual stress, strain and stress fields, crystallographic textures *etc.*, at atomic and crystalline levels. Their measurement and detection principles are similar, mainly depending on scattering techniques, see Figure 11. The incident light beams (monochromatic or white) are directed onto a sample, the scattered beams are captured by the detectors as a function of momentum transfer and/or transferred energy ΔE [213]. Diffraction patterns from a material in (a), can be used to characterise the crystalline structure, residual stress, and crystallographic textures; in (b), small-angle scattering (SAS) uses smaller scattering angles than (a) to investigate material structures with various substances to provide quantitative statistical information at nanoscale levels; in (c), reflectometry is used to study the surface morphology of thin films or multi-layered composites *etc.* [214]; in (d), spectroscopy is performed to determine electronic, vibrational or magnetic excitations, and diffusional processes in solids and liquids.

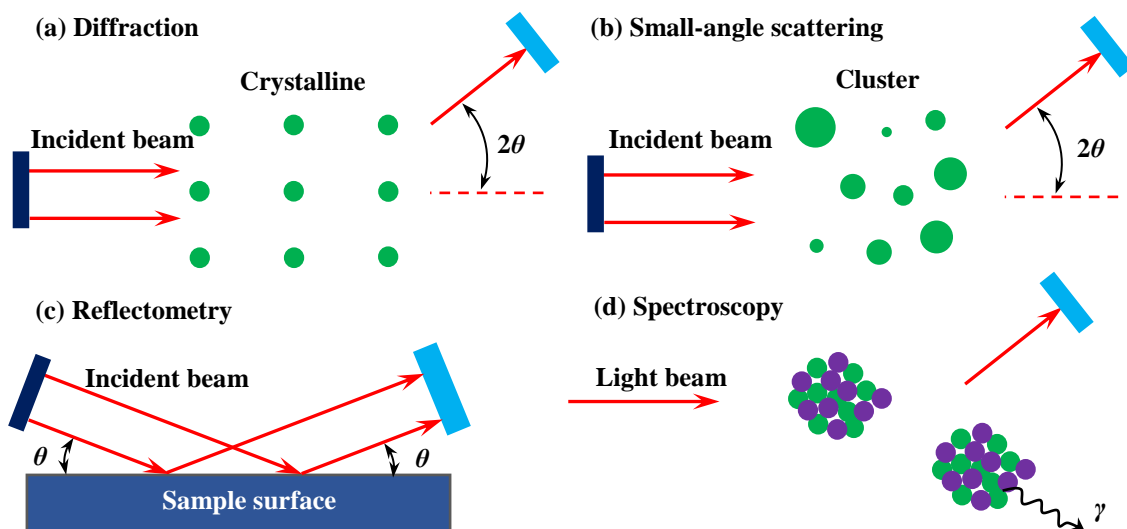


Figure 11 Schematic of synchrotron and neutron measurement techniques: (a) diffraction; (b) small-angle scattering; (c) reflectometry; (d) spectroscopy.

Although synchrotron and neutron imaging share basic principles, the neutron technique is superior in terms of penetration depth; i.e. X-rays (photons) can only be used non-

destructively for examination in the near-surface regions [215]. Neutrons carry no electric charge, so there is no electrostatic interaction with the electron cloud of an atom [213]. The characterisation and analysis of residual stresses in materials science, by using synchrotron and neutron radiation has been documented by Fitpatrick and Lodini [213], and Hutchings *et al.* [216]. Also Banhard *et al.* [212] have reviewed the applications of X-ray and neutron imaging to materials science and engineering.

3.8.1 X-ray imaging

A commonly used laboratory-based X-ray source for imaging is the X-ray tube, as schematically illustrated in Figure 12. A bias voltage of 30-60 kV is applied between the filament and metallic target in an evacuated X-ray tube, causing electrons emitted from the filament to collide with the metallic target at high velocity (energy) and radiate X-rays. The wavelengths of the X-rays are about 0.5-2.5 Å, and depend on the target material. The most commonly used metallic target is copper, which emits strong X-rays with a wavelength of 1.54 Å [217]. Laboratory X-ray imaging (XRI) systems are usually cheaper and easier to access, and are suitable for materials with higher phase contrast, such as glass fibre reinforced composites. The acquisition time for laboratory XRI ranges from minutes at low resolution (sub-millimetre) to hours or even days at high resolution (sub-micron) [218].

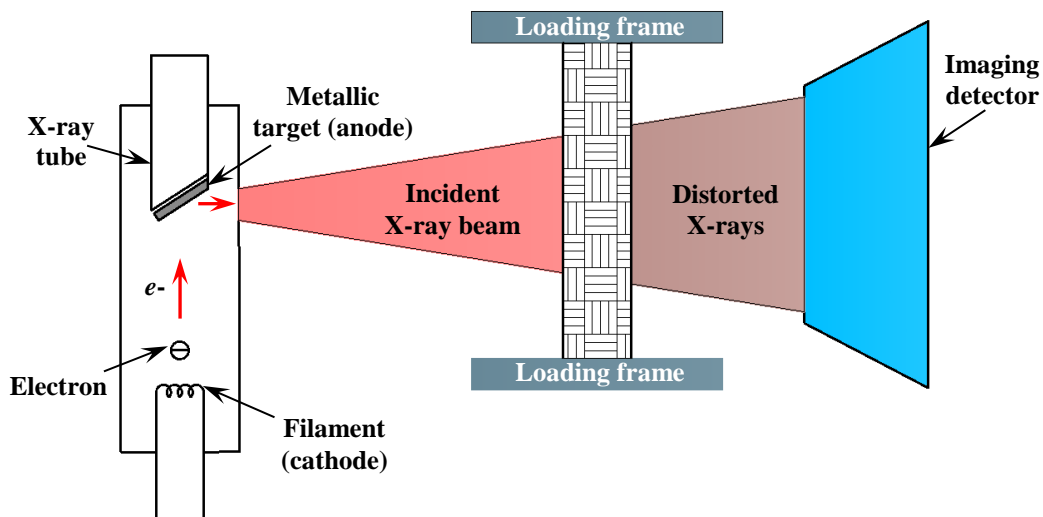


Figure 12 Schematic representation of laboratory-based X-ray imaging.

A major disadvantage of laboratory XRI systems is the lack of capability to penetrate deeply into engineering materials, which depends on X-ray energy and wavelength [216].

Although gamma-rays have higher penetrating capacity than X-rays, they are usually generated from a radioactive source, which cannot be turned off and is difficult to adopt as a compact source to provide a photon flux comparable to an X-ray tube; thus detection efficiency is fairly low and long measuring times are required [219].

The limitations on penetration depth have been overcome by the rapid development of synchrotron facilities. Laboratory X-ray sources produce polychromatic and divergent X-ray beams, while a synchrotron X-ray beam is parallel, monochromatic, more coherent, with higher orders of flux and brightness. These factors determine the image quality and acquisition time. A synchrotron XRI system offers much higher levels of both signal-to-noise ratio and phase contrast, which makes it superior for low contrast materials, such as carbon fibre reinforced composites. The high flux and brilliance of the X-ray beam allows very fast imaging acquisition with high resolution; *e.g.* 1 tomogram per second with 1.1 μm spatial resolution using the TOMCAT beamline at the Swiss Light Source facility [220].

Synchrotron facilities have gone through four generations of technical evolution. The first-generation synchrotron facility was built in the US in 1946 and was primarily used for high-energy particle physics. Second-generation synchrotrons were dedicated to the production of synchrotron light in the 1980s, which used bending magnets to generate synchrotron light. Third-generation light sources originated in the 1990s [221], with facilities that used insertion devices (wigglers and undulators) to produce intense and tuneable X-ray beams. Fourth-generation facilities will be based on free electron lasers which offer more advanced capabilities to generate brighter light sources [222]. Currently, there are about 50 synchrotron facilities around the world, supporting various investigations in engineering, health and medicine, materials science, chemistry, cultural heritage, environmental science and many more [222–231]. Table 7 summarises the 3rd- and 4th-generation synchrotron light source facilities throughout the world. Given that the first 3rd-generation synchrotron facilities were built in 1993, some will be subjected to upgrading in the near future [231].

XRI can also be implemented through different methods as recently presented by Liu *et al.* [210]; Garcea *et al.* reviewed the applications of X-ray computed tomography (CT) to polymer composites [218]. Standard practice in using computed radiography (X-rays or γ -rays) for metallic and non-metallic materials is recommended in ASTM E2033 [232]; ASTM



E2662 provides guidance on the radiographic examination of flat composite panels and sandwich core materials for aerospace applications [233].

Table 7 Summary of third and fourth-generation synchrotron light sources in operation and under construction world-wide; brilliance (brightness) is shown in photons/s/mrad²/mm²/0.1%bw.

| Country | Location | Source | Energy (GeV) | Brilliance | Circumference (m) | Beamlines | Operation year/status |
|-------------|-------------|-----------|--------------|------------------|-------------------|-----------|-----------------------|
| US | Berkeley | ALS | 1.9 | 10 ¹⁹ | 196.8 | 40 | 1993 |
| Italy | Basovizza | ELETTRA | 2.0/2.4 | 10 ¹⁹ | 259.2 | 28 | 1994 |
| France | Grenoble | ESRF | 6.0 | 10 ¹⁹ | 844 | 56 | 1994 |
| China | Taiwan | TLS | 1.5 | 10 ¹⁷ | 120 | 25 | 1994 |
| Korea | Pohang | PLS | 3.0 | 10 ²⁰ | 281.82 | 36 | 1995 |
| US | Lemont | APS | 7.0 | 10 ¹⁴ | 1104 | 68 | 1995 |
| Japan | Hyogo | SPing8 | 8.0 | 10 ²⁰ | 1436 | 62 | 1997 |
| Germany | Berlin | BESSY II | 1.7 | 10 ¹⁹ | 240 | 46 | 1999 |
| Canada | Saskatoon | CLS | 2.9 | 10 ²⁰ | 171 | 22 | 1999 |
| Switzerland | Villigen | SLS | 2.4 | 10 ²⁰ | 288 | 16 | 2001 |
| US | Menlo Park | SPEAR3 | 3.0 | 10 ²⁰ | 234 | 30 | 2004 |
| UK | Didcot | DLS | 3.0 | 10 ²⁰ | 561.6 | 39 | 2006 |
| France | Saint-Aubin | SOLEIL | 2.75 | 10 ¹⁹ | 354 | 29 | 2006 |
| Australia | Clayton | AS | 3.0 | 10 ¹² | 216 | 10 | 2007 |
| China | Beijing | BEPC II | 2.0 | 10 ¹³ | 240 | 14 | 2008 |
| Germany | Hamburg | PETRA III | 6.0 | 10 ²¹ | 2304 | 21 | 2009 |
| China | Shanghai | SSRF | 3.5 | 10 ²⁰ | 432 | 31 | 2009 |
| Spain | Barcelona | ALBA | 3.0 | 10 ²⁰ | 268.8 | 9 | 2012 |
| US | Upton | NSLS-II | 3.0 | 10 ²¹ | 792 | 28 | 2014 |
| China | Taiwan | TPS | 3.0 | 10 ²¹ | 518.4 | 7 | 2016 |
| Krakow | Poland | SOLARIS | 1.5 | 10 ¹⁸ | 96 | 2 | 2016 |
| Jordan | Allan | SESAME | 2.5 | 10 ¹⁸ | 133 | 7 | 2017 |
| Germany | Schenefeld | XFEL | 17.5 | 10 ³³ | 1700 | 6 | 2017 |
| US | Ithaca | CHSS-U | 6.5 | 10 ²¹ | 768.4 | 11 | 2018 |
| Sweden | Lund | MAX IV | 3.0 | 10 ²² | 528 | 17 | 2019 |
| France | Grenoble | ESRF-EBS | 6.0 | 10 ²¹ | 844 | 8 | Under construction |
| Brazil | Campinas | SIRIUS | 3.0 | 10 ²¹ | 518.4 | 13 | Under construction |
| China | Beijing | HEPS | 6.0 | 10 ²² | 1360 | 14 | Under construction |

3.8.2 Neutron imaging

The neutron was discovered by Sir James Chadwick at Cambridge in 1932 [234] through the collision of beryllium by α -particles from polonium. Neutrons have a wave character, their wave-lengths are in the order of interatomic distances (~ 0.1 nm), and kinetic energies close to



atomic vibration energies ($\sim 10^{-2}$ eV). Thus, they give rise to the possibilities of diffraction and inelastic scattering studies, which were experimentally demonstrated in 1946 by Wollan and Clifford using the Graphite Reactor at Oak Ridge National Laboratory, in the era of the Manhattan project in the US [213]. Important progress was made on neutron strain scanning (NSS) during the 1960s and 1970s. Techniques such as small-angle neutron scattering (SANS), neutron time-of-flight (TOF) scattering, backscattering or spin-echo techniques and neutron reflectivity subsequently broadened the applications of NSS to larger scientific domains such as solid state chemistry, liquids, soft matter, materials science, geosciences and biology [235].

A schematic example of NSS using ENGIN-X (ISIS Neutron and Muon Source, Rutherford Appleton Laboratory, UK) is presented in Figure 13 [236]. The pulsed neutron beam with a wide range of energy travels to the sample and, being scattered, the detectors then collect the diffracted neutrons at a fixed angle of $2\theta_b$. As neutrons can penetrate deeply into composite materials, strain/stress can be non-destructively measured [237]. Neutrons are difficult and expensive to produce – neutron sources are usually generated through either nuclear fission reactors (continuous neutron sources) or neutron spallation (pulsed neutron sources). Neutron source facilities are summarised chronologically in Table 8 [213,238,239].

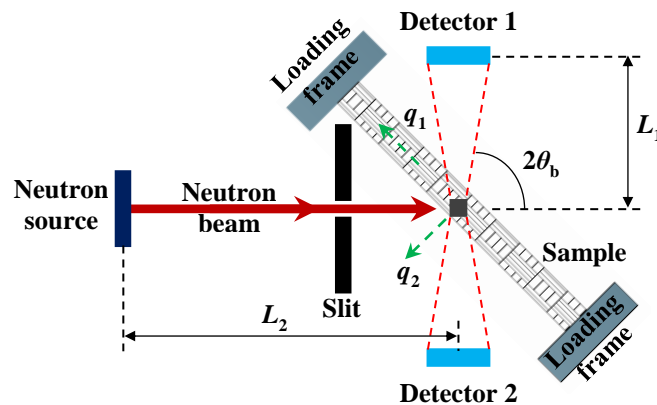


Figure 13 Schematic representation of a time-of-flight neutron strain scanner at the ENGIN-X. The elastic strain is measured along the directions of the impulse exchange vectors, q_1 and q_2 , through the two detectors.

Neutron imaging (NI) has progressed as a reliable NDT technique, in the forms of neutron topography and radiography; specialised instrumentation at pulsed neutron sources include RADEN@J-PARC [240] and IMAT@ISIS [241]. Neutron tomography allows 2D or 3D imaging of the attenuation coefficient distribution within a material system, thus internal

structures and material composition can be visualised [242]; neutron radiography is a transmission imaging technique for heterogeneous materials, taking advantage of the scattering and/or absorption contrast between different elements [243].

Table 8 Summary of neutron source facilities world-wide and their basic parameters.

| Country | Location | Source | First open | Power (MW) | Flux (10^{14} n/cm ² /s) | Scattering instruments | Operating time (d/year) |
|-----------------------------------|---------------|-----------|------------|------------|--|------------------------|-------------------------|
| <i>Continuous neutron sources</i> | | | | | | | |
| Canada | Chalk River | NRU | 1957 | 120 | 3.0 | 6 | 300 |
| Australia | Lucas Heights | HIFAR | 1958 | 10 | 1.4 | 7 | 300 |
| Hungary | Budapest | BNC | 1959 | 10 | 1.6 | 7 | 200 |
| Russia | Gatchina | WWR-M | 1959 | 16 | 1.0 | 12 | 200 |
| Denmark | Risø | DR3 | 1960 | 10 | 1.5 | 7 | 286 |
| Sweden | Studsvik | R-2 | 1960 | 50 | 4.0 | 8 | 187 |
| Japan | Tokai | JRR-3 | 1962 | 20 | 2.0 | 23 | 182 |
| Germany | Juelich | FRJ-2 | 1962 | 23 | 2.0 | 16 | 200 |
| Netherlands | Delft | HOR | 1963 | 2 | 0.2 | 11 | 160 |
| US | Brookhaven | HFBR | 1965 | 30 | 4.0 | 14 | 260 |
| US | Columbia | MURR | 1966 | 10 | 6 | 4 | 338 |
| Russia | Ekaterinburg | IWW-2M | 1966 | 15 | 2.0 | 6 | 250 |
| US | Oak Ridge | HFIR | 1966 | 85 | 25.0 | 14 | 210 |
| Norway | Kjeller | JEEP2 | 1967 | 2 | 0.22 | 8 | 269 |
| US | Gaithersburg | NBSR/NIST | 1969 | 20 | 2.0 | 17 | 250 |
| France | Grenoble | HFR-ILL | 1972 | 58 | 12.0 | 32 | 225 |
| Germany | Berlin | BER-2 | 1973 | 10 | 2.0 | 16 | 240 |
| France | Saclay | Orphée | 1980 | 14 | 3.0 | 25 | 240 |
| Russia | Moscow | IR-8 | 1981 | 8 | 1.0 | 10 | -- |
| US | Sacramento | MNRC | 1990 | 2 | 0.1 | 5 | 50 |
| Switzerland | Villigen | SINQ | 1996 | 1 | 2.0 | 22 | 250 |
| Korea | Taejon | Hanaro | 1996 | 30 | 2.8 | 6 | 252 |
| Australia | Lucas Heights | OPAL | 2007 | 20 | 1.0 | 15 | 300 |
| <i>Pulsed neutron sources</i> | | | | | | | |
| US | Argonne | IPNS | 1980 | 7 | 5 | 13 | 147 |
| Japan | Tsukuba | KENS-KEK | 1980 | 3 kW | 3.0 | 16 | 80 |
| Russia | Dubna | IBR2 | 1984 | 2 | 100 | 13 | 104 |
| UK | Didcot | ISIS | 1985 | 160 kW | 20-100 | 28 | 141 |
| US | Los Alamos | LANSCÉ | 1985 | 56 | 34 | 7 | 100 |
| US | Bloomington | LENS | 2004 | 6 kW | 0.001 | 3 | -- |
| US | Oak Ridge | SNS | 2006 | 1 | 1.5 | 19 | 240 |
| Japan | Tokai | J-PARC | 2007 | 1 | 0.8 | 1 | -- |
| China | Dongguan | CSNS | 2018 | 0.1 | 0.01 | 18 | Under construction |
| ERIC | Lund | ESS | 2023 | 5 | -- | 15 | Under construction |



NI offers a typical spatial resolution of a few hundred microns [244] and below 10 micron in the best case [245]. Although XRI is able to provide sub-micron resolution, NI offers better sensitivity to light elements, especially hydrogen [245]. In terms of efficiency, NI may take several hours (days) compared to minutes or even seconds for XRI; this is due to the low neutron flux, dependency on the number of slices/rotation steps and the materials under investigation. The fundamentals, instrumentation and early applications of neutron imaging are covered by Strobl *et al.* [246]; for recent advances and applications refer to Kardjilov *et al.* [247] and Woracek *et al.* [245].

4 Conclusions and outlook

NDT techniques are invaluable as tools for testing and evaluation, as may be required during various stages within the lifetime of a composite product. It is clear that each technique has its own potential but rarely achieves the capabilities for a full-scale diagnosis of possible defects and damage evolution in a composite system. Table 9 presents the benefits and limitations of the reviewed NDT methods. Appropriate selection of a suitable NDT technique can be challenging but is clearly essential to provide appropriate information for maintaining the structural integrity of composite materials and structures.

Table 9 Benefits and limitations of established non-destructive testing techniques used in composite research.

| NDT technique | Benefits | Limitations | Ref |
|---------------|--|---|--------------|
| VI | Simple, rapid, low cost, easy handling | Only for surface flaws or damage Micro-defects are hardly detected Highly subjective, low repeatability and high reproducibility errors Multiple engineering approaches need to be applied for subsurface flaws | [88] |
| AE | Provide real-time monitoring on growing flaws and damage Highly sensitive to stress waves Suitable for <i>in-situ</i> and field tests Cover large measurement volumes | Specimen must be stressed Sensitivity is affected by surrounding noise Not suitable for thick specimen Difficult to interpret and characterise damage modes High cost of equipment and consumables High acquisition rates and measurements on test specimen are critical | [3,54,56,57] |



| | | | |
|-----|--|---|-------------------|
| UT | <p>Suitable for various material systems Able to detect, locate and size internal flaws Allows one-sided inspection Rapid scan and long-range inspection Good for assembly lines Compact and portable equipment, suitable for on-site inspection Often cost-effective Non-ionizing radiation</p> | <p>Complex setup and transducer design Need skills and experience on multi-modes and complex features Sensitive to operational and environmental surroundings Hard to detect defects near probe Resolution may be limited by algorithms and computing power</p> | [79,85] |
| IRT | <p>Real-time and large-field visual presentation of defects Suitable for wide selection of materials Allows one-sided inspection Safe and easy to operate Cost-effective and productive Non-ionizing radiation</p> | <p>Vulnerable and sensitive for <i>in-situ</i> and field tests Limited by cost and availability of excitation sources in field Reduced accuracy with complex geometries Data processing is time-consuming; depends on computing power and algorithms</p> | [100,106,127,248] |
| THz | <p>Robust and repeatable, high scan rate with imaging High precision, sensitivity and resolution High penetration depths for most composites Non-ionizing radiation</p> | <p>Low speed of examination Restricted to nonconductive materials Costly</p> | [2,47,146] |
| ST | <p>Non-contact and full-field surface strain measurement More resilient to environmental disturbance Suitable for large composite structures Efficient for high speed, automated inspection in production environments</p> | <p>External excitation sources are required Limited tolerance to rigid-body motion Limited capabilities for subsurface damage detection Accuracy depends on various sources of uncertainties</p> | [49,158,178] |
| DIC | <p>Cost-effective and easy implementation Adjustable spatial and temporal resolution Insensitive to ambient variations</p> | <p>Speckle patterns are required with high quality Accuracy depends on speckle pattern Limited capability for subsurface detection</p> | [196,197] |
| XRI | <p>Suitable for various materials and <i>in-situ</i> tests Can detect both surface and bulk defects 2D and 3D images reveal very detailed shape of defects Special resolution at sub-micron level High efficiency Extensive image processing capability</p> | <p>Not suitable for large size structures Not suitable for in-field tests Access to both sides required Dangerous ionizing radiation, requires protection Facilities and access are limited</p> | [212,218,249] |
| NI | <p>Suitable for various materials and <i>in-situ</i> tests Can detect both surface and bulk defects 2D and 3D images reveal the nature and detailed shape of defects Special resolution at sub-millimetre level Extensive image processing capability Penetration depth greater than X-rays High sensitivity to light elements</p> | <p>Not suitable for in-field tests Access to both sides required Dangerous ionizing radiation, requires protection Acquisition efficiency lower than XRI Facilities and access are limited and more expensive than XRI</p> | [212,245,247] |



The applications and capabilities of each reviewed NDT technique for detection and evaluation of defects and damage evolution in composite materials/structures are summarised in Table 10. As the volume and structural complexity of composite parts continue to grow, the uses of multi-NDT techniques are becoming increasingly popular in maintaining structural integrity; research in this approach is also growing rapidly.

Table 10 Applications and capabilities of established NDT techniques for composite inspection and evaluation.

| Defects/damages | AE | UT | IRT | THz | ST | DIC | XRI | NI |
|--|------------|------------|------------|----------------|---------------|-------|-------|------------|
| <i>Manufacturing induced flaws/defects</i> | | | | | | | | |
| Surface defects | | | [250] | [251] | [252] | | [253] | |
| Subsurface defects | [254] | [255, 256] | [250, 257] | [141,145, 251] | [153,25 8] | | [259] | [260, 261] |
| Delamination | [262] | [263] | [263] | [264] | [265] | [266] | | |
| Location of depth/size | | [267] | [268] | [90] | [153] | | [267] | |
| Interface debonding | [70] | [269] | [270] | [271] | | | [272] | |
| Fibre content and orientation | | [31] | [273] | [141] | | [274] | [275] | [276] |
| Cracks, fibre breakage/fracture | [277, 278] | [279] | [280] | [141] | [191] | [203] | [281] | [282] |
| Moisture, liquids, or voids | | | [283] | [284] | [154] | | [285] | [286, 287] |
| Shape/surface profiling | | | | | [168] | | | |
| <i>In-service/in-situ detection</i> | | | | | | | | |
| Impact damage | | [91,2 88] | [112] | [289] | [91,156 ,172] | [290] | [290] | |
| Tensile cracking/damage | [278, 291] | | | | | [207] | [292] | [292] |
| Compressive failure | | | [293] | | | [293] | | |
| Bending fatigue damage | [294] | | | [295] | | [294] | [294] | |
| Tensile-tensile fatigue | [296] | | | | | [199] | [297] | [298] |
| Structural damage monitoring | [299] | | [300] | [301] | | [302] | | |
| Quantitative strain monitoring | | | | | [303] | [202] | [304] | [237] |
| Mechanical analysis | | | | | [166,16 7] | [206] | | |
| Hygrothermal damage | | | | [305] | | | [306] | |

The initial development and application of various NDT techniques are driven by demands from aerospace industries, which rapidly expand to other fields. AE, ultrasound, IRT, shearography, DIC and X-ray imaging represent the main techniques within composite industries, and continue to play essential roles especially in aerospace, automotive, marine and construction applications. NDT techniques based on ultrasound, IRT and DIC are versatile and cost-effective solutions, which have been used extensively in many industrial fields, as well as academic research tools. THz waves can pass through opaque materials and detect internal



defects and damage; thus it is a promising NDT technique, possessing great potential in the near future. Innovation and development of compact and portable NDT devices will continue to have a major role for future NDT equipment as these will offer in-service or *in-situ* inspections to facilitate the decision making process.

Considering the complex nature of defects and damage detection in composites, the future development of NDT techniques will increasingly depend on intelligent and automated inspection systems with high accuracy and efficiency in data processing. Machine Learning and deep learning provides significant potential for the NDT evaluation of composite materials – artificial intelligence based approaches offer fast decision making without human interference. Various automated diagnostic systems have been proposed for different NDT techniques to offer fast and accurate analysis. These are achieved through artificial neural network coding or algorithms to enable automatic detection and recognition of defects/damage. Examples include: applying pattern recognition to discriminate failure modes in composites using acoustic emission data [307]; damage classification in CFRP laminates using artificial neural networks in ultrasonic testing [308]; automatic defect detection through infrared thermography in CFRP laminates [309] and honeycomb composite structures [310]; an automated shearography system for cylindrical surface inspection using machining learning [252]; neural network-based hybrid signal processing for terahertz pulsed imaging [311]. Despite the exciting achievements in NDT techniques, there is still substantial work required to develop fast and affordable systems for both equipment and data processing methods to promote their practical implementation in industry.

Although X-ray and neutron imaging are powerful tools for NDT tests offering super high resolution, both imaging techniques are based on ionizing radiation; *i.e.* specimens have to be analysed using radiation facilities which are inconvenient compared to other NDT techniques. Also, locations and availability of synchrotron facilities are very limited, which further constrain their accessibility and costs. Portable X-ray or neutron generators have been commercialised to provide easier access. Whilst they have found applications in aerospace, marine, construction and pipeline inspection, their capabilities for composite industries are limited. The use of neutron imaging depends on advances in neutron production and instrumentation, whilst its research community is growing rapidly. Free electron lasers and



modern spallation sources are promising techniques that should enhance the future development of NDT technology towards more advanced capabilities.

Funding

The author(s) received no financial support for the research, authorship, and/or publication of this article.

Declaration of conflicting interests

The author(s) declared no potential conflicts of interest with respect to the research, authorship, and/or publication of this article.

References

- [1] Ashby MF, Cebon D. Materials selection in mechanical design. *Le J Phys IV* 1993; 3: C7-1.
- [2] Amenabar I, Lopez F, Mendikute A. In introductory review to THz non-destructive testing of composite mater. *J Infrared, Millimeter, Terahertz Waves* 2013; 34: 152–69.
- [3] Hamstad MA. A review: acoustic emission, a tool for composite-materials studies. *Exp Mech* 1986; 26: 7–13.
- [4] Duchene P, Chaki S, Ayadi A, Krawczak P. A review of non-destructive techniques used for mechanical damage assessment in polymer composites. *J Mater Sci* 2018; 53: 7915–38.
- [5] ASTM International. Standard guide for nondestructive testing of polymer matrix composites used in aerospace applications - E2533 2017:1–48. doi:10.1520/E2533-17E01.
- [6] Summerscales J. *Non-destructive testing of fibre-reinforced plastics composites*. vol. 2. Springer Science & Business Media; 1990.
- [7] Birt EA, Smith RA. A review of NDE methods for porosity measurement in fibre-reinforced polymer composites. *Insight-Non-Destructive Test Cond Monit* 2004; 46: 681–6.



- [8] Cheng L, Tian GY. Comparison of nondestructive testing methods on detection of delaminations in composites. *J Sensors* 2012;2012:1–7.
- [9] Heuer H, Schulze M, Pooch M, Gäbler S, Nocke A, Bardl G, et al. Review on quality assurance along the CFRP value chain—non-destructive testing of fabrics, preforms and CFRP by HF radio wave techniques. *Compos Part B Eng* 2015;77:494–501.
- [10] Li Z, Meng Z. A review of the radio frequency non-destructive testing for carbon-fibre composites. *Meas Sci Rev* 2016;16:68–76.
- [11] Gholizadeh S. A review of non-destructive testing methods of composite materials. *Procedia Struct Integr* 2016;1:50–7.
- [12] Guo N, Cawley P. The non-destructive assessment of porosity in composite repairs. *Composites* 1994;25:842–50.
- [13] Naebe M, Abolhasani MM, Khayyam H, Amini A, Fox B. Crack Damage in Polymers and Composites: A Review. *Polym Rev* 2016;56:31–69.
- [14] Asif M, Khan MA, Khan SZ, Choudhry RS, Khan KA. Identification of an effective nondestructive technique for bond defect determination in laminate composites—A technical review. *J Compos Mater* 2018;52:3589–99.
- [15] Jolly MR, Prabhakar A, Sturzu B, Hollstein K, Singh R, Thomas S, et al. Review of non-destructive testing (NDT) techniques and their applicability to thick walled composites. *Procedia CIRP* 2015;38:129–36.
- [16] Hsu DK. Nondestructive Evaluation of Sandwich Structures: A Review of Some Inspection Techniques. *J Sandw Struct Mater* 2009;11:275–91.
- [17] Ibrahim ME. Nondestructive evaluation of thick-section composites and sandwich structures: A review. *Compos Part A Appl Sci Manuf* 2014;64:36–48.
- [18] Cawley P. The rapid non-destructive inspection of large composite structures. *Composites* 1994;25:351–7.
- [19] Mook G, Pohl J, Michel F. Non-destructive characterization of smart CFRP structures. *Smart Mater Struct* 2003;12:997–1004.
- [20] Zou Y, Tong L, Steven GP. Vibration-based model-dependent damage (delamination) identification and health monitoring for composite structures—a review. *J Sound Vib* 2000;230:357–78.
- [21] Tuloup C, Harizi W, Aboura Z, Meyer Y, Khellil K, Lachat R. On the use of in-situ piezoelectric sensors for the manufacturing and structural health monitoring of polymer-matrix composites: A literature review. *Compos Struct* 2019;215:127–49.
- [22] Greene E. Marine composites non-destructive evaluation. *Sh Struct* 2014;1:416–27.



- [23] Drewry MA, Georgiou GA. A review of NDT techniques for wind turbines. *Insight-Non-Destructive Test Cond Monit* 2007;49:137–41.
- [24] Ciang CC, Lee J-R, Bang H-J. Structural health monitoring for a wind turbine system: a review of damage detection methods. *Meas Sci Technol* 2008;19:122001.
- [25] Raišutis R, Jasiūnienė E, Šliteris R, Vladišauskas A. The review of non-destructive testing techniques suitable for inspection of the wind turbine blades. *Ultragarsas* 2008;63:26–30.
- [26] Galappaththi UIK, De Silva AKM, Macdonald M, Adewale OR. Review of inspection and quality control techniques for composite wind turbine blades. *Insight-Non-Destructive Test Cond Monit* 2012;54:82–5.
- [27] Garnier C, Pastor M-L, Eyma F, Lorrain B. The detection of aeronautical defects in situ on composite structures using Non Destructive Testing. *Compos Struct* 2011;93:1328–36.
- [28] Katnam KB, Da Silva LFM, Young TM. Bonded repair of composite aircraft structures: A review of scientific challenges and opportunities. *Prog Aerosp Sci* 2013;61:26–42.
- [29] Fahr A. Aeronautical applications of non-destructive testing. DEstech Publications, Inc; 2013.
- [30] Joyce PJ, Kugler D, Moon TJ. A technique for characterizing process-induced fiber waviness in unidirectional composite laminates-using optical microscopy. *J Compos Mater* 1997;31:1694–727.
- [31] Pain D, Drinkwater BW. Detection of Fibre Waviness Using Ultrasonic Array Scattering Data. *J Nondestruct Eval* 2013;32:215–27.
- [32] Hull D, Clyne TW. An introduction to composite materials. Cambridge university press; 1996.
- [33] Wang B, Fancey KS. Viscoelastically prestressed polymeric matrix composites: An investigation into fibre deformation and prestress mechanisms. *Compos Part A Appl Sci Manuf* 2018;111:106–14.
- [34] Wang J, Potter KD, Hazra K, Wisnom MR. Experimental fabrication and characterization of out-of-plane fiber waviness in continuous fiber-reinforced composites. *J Compos Mater* 2012;46:2041–53.
- [35] Hyer MW. Some Observations on the Cured Shape of Thin Unsymmetric Laminates. *J Compos Mater* 1981;15:175–94.
- [36] Hyer MW. The Room-Temperature Shapes of Four-Layer Unsymmetric Cross-Ply Laminates. *J Compos Mater* 1982;16:318–40.



- [37] Wang B, Fancey KS. A bistable morphing composite using viscoelastically generated prestress. *Mater Lett* 2015;158:108–10.
- [38] Wang B, Ge C, Fancey KS. Snap-through behaviour of a bistable structure based on viscoelastically generated prestress. *Compos Part B Eng* 2017;114:23–33.
- [39] Lubin G. *Handbook of composites*. Springer Science & Business Media; 2013.
- [40] Berthelot JM, Rhazi J. Acoustic emission in carbon fibre composites. *Compos Sci Technol* 1990;37:411–28.
- [41] Haque A, Hossain MK. Effects of moisture and temperature on high strain rate behavior of S2-Glass–Vinyl ester woven composites. *J Compos Mater* 2003;37:627–47.
- [42] Huang S, Wang S. *New technologies in electromagnetic non-destructive testing*. Springer; 2016.
- [43] Ghoni R, Dollah M, Sulaiman A, Ibrahim FM. Defect Characterization Based on Eddy Current Technique: Technical Review. *Adv Mech Eng* 2014;6:182496. doi:10.1155/2014/182496.
- [44] Koyama K, Hoshikawa H, Kojima G. Eddy Current Nondestructive Testing for Carbon Fiber- Reinforced Composites. *J Press Vessel Technol* 2013;135:041501.
- [45] Ferguson B, Zhang X-C. Materials for terahertz science and technology. *Nat Mater* 2002;1:26–33.
- [46] Dhillon SS, Vitiello MS, Linfield EH, Davies AG, Hoffmann MC, Booske J, et al. The 2017 terahertz science and technology roadmap. *J Phys D Appl Phys* 2017;50:43001.
- [47] Zhong S. Progress in terahertz nondestructive testing: A review. *Front Mech Eng* 2019;14:273–81.
- [48] Ambrosini D, Ferraro P. Here, there and everywhere: The art and science of optics at work. *Opt Lasers Eng* 2018;104:1–8.
- [49] Hung YY, Ho HP. Shearography: An optical measurement technique and applications. *Mater Sci Eng R Reports* 2005;49:61–87.
- [50] Yang L, Xie X. *Digital shearography: New developments and applications*. vol. 31. SPIE Press Bellingham; 2016.
- [51] Arai M, Crawford K. Neutron sources and facilities. *Neutron imaging Appl.*, Springer; 2009, p. 13–30.
- [52] Meola C, Carlomagno GM. Application of infrared thermography to adhesion science. *J Adhes Sci Technol* 2006;20:589–632.
- [53] Schoonahd JW, Gould JD, Miller LA. Studies of visual inspection. *Ergonomics* 1973;16:365–79.



- [54] Scruby CB. An introduction to acoustic emission. *J Phys E* 1987;20:946–53.
- [55] Kaiser J. An investigation into the occurrence of noises in tensile tests or a study of acoustic phenomena in tensile tests. Ph. D. Dissertation Technische Hochschule Munchen, Munich, 1950.
- [56] Tensi HM. The Kaiser-effect and its scientific background. *J Acoust Emiss* 2004;22:s1–16.
- [57] Dahmene F, Yaacoubi S, Mountassir MEL. Acoustic emission of composites structures: story, success, and challenges. *Phys Procedia* 2015;70:599–603.
- [58] Huguet S, Godin N, Gaertner R, Salmon L, Villard D. Use of acoustic emission to identify damage modes in glass fibre reinforced polyester. *Compos Sci Technol* 2002;62:1433–44.
- [59] Godin N, Huguet S, Gaertner R, Salmon L. Clustering of acoustic emission signals collected during tensile tests on unidirectional glass/polyester composite using supervised and unsupervised classifiers. *NDT E Int* 2004;37:253–64.
- [60] Kordatos EZ, Dassios KG, Aggelis DG, Matikas TE. Rapid evaluation of the fatigue limit in composites using infrared lock-in thermography and acoustic emission. *Mech Res Commun* 2013;54:14–20.
- [61] Nechad H, Helmstetter A, El Guerjouma R, Sornette D. Creep Ruptures in Heterogeneous Materials. *Phys Rev Lett* 2005;94:45501.
- [62] Chou HY, Mouritz AP, Bannister MK, Bunsell AR. Acoustic emission analysis of composite pressure vessels under constant and cyclic pressure. *Compos Part A Appl Sci Manuf* 2015;70:111–20.
- [63] Barré S, Benzeggagh ML. On the use of acoustic emission to investigate damage mechanisms in glass-fibre-reinforced polypropylene. *Compos Sci Technol* 1994;52:369–76.
- [64] ASTM International. Standard practice for acoustic emission examination of fiberglass reinforced plastic resin (FRP) tanks/vessels - E1067 2018:1–16.
- [65] ASTM International. Standard practice for acoustic emission examination of reinforced thermosetting resin pipe (RTRP) - E1118 2016:1–13.
- [66] ASTM International. Standard practice for examination of gas-filled filament-wound composite pressure vessels using acoustic emission - E2191 2016:1–9.
- [67] ASTM International. Standard practice for examination of fiberglass reinforced plastic fan blades using acoustic emission - E2076 2015:1–6.
- [68] ASTM International. Standard practice for acoustic emission examination of plate-like



- and flat panel composite structures used in aerospace applications - *E2661* 2015:1–19.
- [69] Ramirez-Jimenez CR, Papadakis N, Reynolds N, Gan TH, Purnell P, Pharaoh M. Identification of failure modes in glass/polypropylene composites by means of the primary frequency content of the acoustic emission event. *Compos Sci Technol* 2004;64:1819–27.
- [70] Marec A, Thomas J-H, El Guerjouma R. Damage characterization of polymer-based composite materials: Multivariable analysis and wavelet transform for clustering acoustic emission data. *Mech Syst Signal Process* 2008;22:1441–64.
- [71] Sikdar S, Mirgal P, Banerjee S, Ostachowicz W. Damage-induced acoustic emission source monitoring in a honeycomb sandwich composite structure. *Compos Part B Eng* 2019;158:179–88.
- [72] Cui X, Yan Y, Ma Y, Ma L, Han X. Localization of CO₂ leakage from transportation pipelines through low frequency acoustic emission detection. *Sensors Actuators A Phys* 2016;237:107–18.
- [73] Schabowicz K, Gorzelańczyk T, Szymków M. Identification of the degree of degradation of fibre-cement boards exposed to fire by means of the acoustic emission method and artificial neural networks. *Materials (Basel)* 2019;12:656.
- [74] Svečko R, Kusić D, Kek T, Sarjaš A, Hančič A, Grum J. Acoustic Emission Detection of Macro-Cracks on Engraving Tool Steel Inserts during the Injection Molding Cycle Using PZT Sensors. *Sensors* 2013;13:6365–79.
- [75] Vary A. Acousto-ultrasonic characterization of fiber reinforced composites. *Mater Eval* 1982;40:1–15.
- [76] Vary A. The acousto-ultrasonic approach. *Acousto-Ultrasonics*, Springer; 1988, p. 1–21.
- [77] Rose JL. A baseline and vision of ultrasonic guided wave inspection potential. *J Press Vessel Technol* 2002;124:273–82.
- [78] Rose JL. *Ultrasonic guided waves in solid media*. Cambridge university press; 2014.
- [79] Felice M V, Fan Z. Sizing of flaws using ultrasonic bulk wave testing: A review. *Ultrasonics* 2018;88:26–42.
- [80] Munian RK, Mahapatra DR, Gopalakrishnan S. Lamb wave interaction with composite delamination. *Compos Struct* 2018;206:484–98.
- [81] Smith RA, Nelson LJ, Mienczakowski MJ, Wilcox PD. Ultrasonic tracking of ply drops in composite laminates. *AIP Conf. Proc.*, vol. 1706, AIP Publishing; 2016, p. 50006.
- [82] Smith RA, Clarke B. Ultrasonic C-scan determination of ply stacking sequence in



- carbon-fibre composites. *Insight* 1994;36:741–7.
- [83] Li C, Pain D, Wilcox PD, Drinkwater BW. Imaging composite material using ultrasonic arrays. *NDT E Int* 2013;53:8–17.
- [84] Su Z, Ye L, Lu Y. Guided Lamb waves for identification of damage in composite structures: A review. *J Sound Vib* 2006;295:753–80.
- [85] Guan R, Lu Y, Duan W, Wang X. Guided waves for damage identification in pipeline structures: A review. *Struct Control Heal Monit* 2017;24:e2007.
- [86] ASTM International. Standard practice for use of the ultrasonic time of flight diffraction (TOFD) technique - E2373 2014:1–13.
- [87] ASTM International. Standard practice for ultrasonic testing of flat panel composites and sandwich core materials used in aerospace applications - E2580 2017:1–7.
- [88] ASTM International. Standard guide for nondestructive testing of the composite overwraps in filament wound pressure vessels used in aerospace applications - E2981 2015:1–36.
- [89] Sherafat MH, Quaegebeur N, Hubert P, Lessard L, Masson P. Experimental Model of Impact Damage for Guided Wave-Based Inspection of Composites. *J Nondestruct Eval Diagnostics Progn Eng Syst* 2018;1:040801.
- [90] Dong J, Kim B, Locquet A, McKeon P, Declercq N, Citrin DS. Nondestructive evaluation of forced delamination in glass fiber-reinforced composites by terahertz and ultrasonic waves. *Compos Part B Eng* 2015;79:667–75.
- [91] Růžek R, Lohonka R, Jironč J. Ultrasonic C-Scan and shearography NDI techniques evaluation of impact defects identification. *NDT E Int* 2006;39:132–42.
- [92] Riise J, Mineo C, Pierce SG, Nicholson PI, Cooper I. Adapting robot paths for automated NDT of complex structures using ultrasonic alignment. *AIP Conf Proc* 2019;2102:40006.
- [93] Kim H, Kim T, Morrow D, Jiang X. Stress Measurement of a Pressurized Vessel Using Ultrasonic Subsurface Longitudinal Wave with 1-3 Composite Transducers. *IEEE Trans Ultrason Ferroelectr Freq Control* 2019:1.
- [94] Derusova DA, Vavilov VP, Sfarra S, Sarasini F, Druzhinin N V. Applying ultrasonic resonance vibrometry for the evaluation of impact damage in natural/synthetic fibre reinforced composites. *Polym Test* 2018;68:70–6.
- [95] Vollmer M, Möllmann K-P. *Infrared thermal imaging: fundamentals, research and applications*. 2nd Editio. John Wiley & Sons; 2017.
- [96] Meola C. *Infrared thermography recent advances and future trends*. Bentham Science



Publishers; 2012.

- [97] Zhu Y-K, Tian G-Y, Lu R-S, Zhang H. A review of optical NDT technologies. *Sensors* 2011;11:7773–98.
- [98] Usamentiaga R, Venegas P, Guerediaga J, Vega L, Molleda J, Bulnes F. Infrared thermography for temperature measurement and non-destructive testing. *Sensors* 2014;14:12305–48.
- [99] Balaras CA, Argiriou AA. Infrared thermography for building diagnostics. *Energy Build* 2002;34:171–83. doi:[https://doi.org/10.1016/S0378-7788\(01\)00105-0](https://doi.org/10.1016/S0378-7788(01)00105-0).
- [100] Bagavathiappan S, Lahiri BB, Saravanan T, Philip J, Jayakumar T. Infrared thermography for condition monitoring—A review. *Infrared Phys Technol* 2013;60:35–55.
- [101] Huda ASN, Taib S. Application of infrared thermography for predictive/preventive maintenance of thermal defect in electrical equipment. *Appl Therm Eng* 2013;61:220–7.
- [102] Lahiri BB, Bagavathiappan S, Jayakumar T, Philip J. Medical applications of infrared thermography: A review. *Infrared Phys Technol* 2012;55:221–35.
- [103] Soroko M, Howell K. Infrared thermography: Current applications in equine medicine. *J Equine Vet Sci* 2018;60:90–6.
- [104] Wiecek B. Review on thermal image processing for passive and active thermography. 2005 IEEE Eng. Med. Biol. 27th Annu. Conf., IEEE; 2006, p. 686–9.
- [105] Theodorakeas P, Cheilakou E, Ftikou E, Kouli M. Passive and active infrared thermography: an overview of applications for the inspection of mosaic structures. *J. Phys. Conf. Ser.*, vol. 655, IOP Publishing; 2015, p. 12061.
- [106] Doshvarpassand S, Wu C, Wang X. An overview of corrosion defect characterization using active infrared thermography. *Infrared Phys Technol* 2019;96:366–89.
- [107] Sun JG. Analysis of pulsed thermography methods for defect depth prediction. *J Heat Transfer* 2006;128:329–38.
- [108] Busse G, Wu D, Karpen W. Thermal wave imaging with phase sensitive modulated thermography. *J Appl Phys* 1992;71:3962–5.
- [109] Li T, Almond DP, Rees DAS. Crack imaging by scanning pulsed laser spot thermography. *NDT E Int* 2011;44:216–25.
- [110] Schlichting J, Maierhofer C, Kreuzbruck M. Crack sizing by laser excited thermography. *NDT E Int* 2012;45:133–40.
- [111] Riegert G, Zweschper T, Busse G. Lockin thermography with eddy current excitation.



- Quant Infrared Thermogr J 2004;1:21–32.
- [112] Pan M, He Y, Tian G, Chen D, Luo F. Defect characterisation using pulsed eddy current thermography under transmission mode and NDT applications. *Ndt E Int* 2012;52:28–36.
- [113] He Y, Pan M, Luo F. Defect characterisation based on heat diffusion using induction thermography testing. *Rev Sci Instrum* 2012;83:104702.
- [114] Liang T, Ren W, Tian GY, Elradi M, Gao Y. Low energy impact damage detection in CFRP using eddy current pulsed thermography. *Compos Struct* 2016;143:352–61.
- [115] Tenek LH, Henneke II EG, Gunzburger MD. Vibration of delaminated composite plates and some applications to non-destructive testing. *Compos Struct* 1993;23:253–62.
- [116] Rantala J, Wu D, Busse G. Amplitude-modulated lock-in vibrothermography for NDE of polymers and composites. *Res Nondestruct Eval* 1996;7:215–28.
- [117] Pieczonka L, Aymerich F, Brozek G, Szewedo M, Staszewski WJ, Uhl T. Modelling and numerical simulations of vibrothermography for impact damage detection in composites structures. *Struct Control Heal Monit* 2013;20:626–38.
- [118] Palumbo D, Ancona F, Galietti U. Quantitative damage evaluation of composite materials with microwave thermographic technique: feasibility and new data analysis. *Meccanica* 2015;50:443–59.
- [119] Foudazi A, Edwards CA, Ghasr MT, Donnell KM. Active microwave thermography for defect detection of CFRP-strengthened cement-based materials. *IEEE Trans Instrum Meas* 2016;65:2612–20.
- [120] Wu D, Busse G. Lock-in thermography for nondestructive evaluation of materials. *Rev Générale Therm* 1998;37:693–703.
- [121] Yang R, He Y. Optically and non-optically excited thermography for composites: A review. *Infrared Phys Technol* 2016;75:26–50.
- [122] ASTM International. Standard practice for infrared flash thermography of composite panels and repair patches used in aerospace applications - E2582 2019:1–6.
- [123] Avdelidis NP, Hawtin BC, Almond DP. Transient thermography in the assessment of defects of aircraft composites. *NDT E Int* 2003;36:433–9.
- [124] Chatterjee K, Tuli S, Pickering SG, Almond DP. A comparison of the pulsed, lock-in and frequency modulated thermography nondestructive evaluation techniques. *NDT E Int* 2011;44:655–67.
- [125] Bolu G, Gachagan A, Pierce G, Harvey G. Reliable thermosonic inspection of aero engine turbine blades. *Insight - Non-Destructive Test Cond Monit* 2010;52:488–93.



- [126] Hu Q, Chen Y, Hong J, Jin S, Zou G, Chen L, et al. A smart epoxy composite based on phase change microcapsules: preparation, microstructure, thermal and dynamic mechanical performances. *Molecules* 2019;24:916.
- [127] Jorge Aldave I, Venegas Bosom P, Vega González L, López de Santiago I, Vollheim B, Krausz L, et al. Review of thermal imaging systems in composite defect detection. *Infrared Phys Technol* 2013;61:167–75.
- [128] Naderi M, Kahirdeh A, Khonsari MM. Dissipated thermal energy and damage evolution of Glass/Epoxy using infrared thermography and acoustic emission. *Compos Part B Eng* 2012;43:1613–20.
- [129] Bailey PBS, Lafferty AD. Specimen gripping effects in composites fatigue testing—Concerns from initial investigation. *Express Polym Lett* 2015;9:480–8.
- [130] Vavilov VP, Plesovskikh A V, Chulkov AO, Nesteruk DA. A complex approach to the development of the method and equipment for thermal nondestructive testing of CFRP cylindrical parts. *Compos Part B Eng* 2015;68:375–84.
- [131] Usamentiaga R, Venegas P, Guerediaga J, Vega L, López I. Feature extraction and analysis for automatic characterization of impact damage in carbon fiber composites using active thermography. *NDT E Int* 2013;54:123–32.
- [132] Meola C, Carlomagno GM. Infrared thermography to evaluate impact damage in glass/epoxy with manufacturing defects. *Int J Impact Eng* 2014;67:1–11.
- [133] Tonouchi M. Cutting-edge terahertz technology. *Nat Photonics* 2007;1:97–105.
- [134] Sirtori C. Bridge for the terahertz gap. *Nature* 2002;417:132–3. doi:10.1038/417132b.
- [135] Auston DH, Cheung KP, Valdmanis JA, Kleinman DA. Cherenkov Radiation from Femtosecond Optical Pulses in Electro-Optic Media. *Phys Rev Lett* 1984;53:1555–8.
- [136] Fattinger C, Grischkowsky D. Point source terahertz optics. *Appl Phys Lett* 1988;53:1480–2.
- [137] Dobroiu A, Otani C, Kawase K. Terahertz-wave sources and imaging applications. *Meas Sci Technol* 2006;17:R161–74.
- [138] Guillet JP, Recur B, Frederique L, Bousquet B, Canioni L, Manek-Hönninger I, et al. Review of terahertz tomography techniques. *J Infrared, Millimeter, Terahertz Waves* 2014;35:382–411.
- [139] Redo-Sanchez A, Heshmat B, Aghasi A, Naqvi S, Zhang M, Romberg J, et al. Terahertz time-gated spectral imaging for content extraction through layered structures. *Nat Commun* 2016;7:12665.
- [140] Wang Q, Zhou H, Liu M, Li X, Hu Q. Study of the skin depth and defect detection in



- carbon fiber composites with Terahertz waves. *Optik (Stuttg)* 2019;178:1035–44.
- [141] Dong J, Pomarède P, Chehemi L, Locquet A, Meraghni F, Declercq NF, et al. Visualization of subsurface damage in woven carbon fiber-reinforced composites using polarization-sensitive terahertz imaging. *NDT E Int* 2018;99:72–9.
- [142] Zhang H, Sfarra S, Sarasini F, Santulli C, Fernandes H, Avdelidis NP, et al. Thermographic non-destructive evaluation for natural fiber-reinforced composite laminates. *Appl Sci* 2018;8:240.
- [143] Han D-H, Kang L-H. Nondestructive evaluation of GFRP composite including multi-delamination using THz spectroscopy and imaging. *Compos Struct* 2018;185:161–75.
- [144] Yahng JS, Park C-S, Don Lee H, Kim C-S, Yee D-S. High-speed frequency-domain terahertz coherence tomography. *Opt Express* 2016;24:1053–61.
- [145] Zhang J, Li W, Cui H-L, Shi C, Han X, Ma Y, et al. Nondestructive evaluation of carbon fiber reinforced polymer composites using reflective terahertz imaging. *Sensors* 2016;16:875.
- [146] Lopato P. Double-sided terahertz imaging of multilayered glass fiber-reinforced polymer. *Appl Sci* 2017;7:661.
- [147] Okano M, Watanabe S. Internal status of visibly opaque black rubbers investigated by terahertz polarization spectroscopy: Fundamentals and applications. *Polymers (Basel)* 2018;11:9.
- [148] Jansen C, Wietzke S, Peters O, Scheller M, Vieweg N, Salhi M, et al. Terahertz imaging: applications and perspectives. *Appl Opt* 2010;49:E48–57.
- [149] Leendertz JA. Interferometric displacement measurement on scattering surfaces utilizing speckle effect. *J Phys E* 1970;3:214–8.
- [150] Leendertz JA, Butters JN. An image-shearing speckle-pattern interferometer for measuring bending moments. *J Phys E* 1973;6:1107–10.
- [151] Chau FS, Toh SL, Tay CJ, Shang HM. Some examples of nondestructive flaw detection by shearography. *J Nondestruct Eval* 1989;8:225–34.
- [152] Toh SL, Shang HM, Chau FS, Tay CJ. Flaw detection in composites using time-average shearography. *Opt Laser Technol* 1991;23:25–30.
- [153] De Angelis G, Meo M, Almond DP, Pickering SG, Angioni SL. A new technique to detect defect size and depth in composite structures using digital shearography and unconstrained optimization. *NDT E Int* 2012;45:91–6.
- [154] Tyson JII, Newman JW. Apparatus and method for detecting leaks in packages. US5307139A, 1994.



- [155] Rubayi NA, Liew SH. Vacuum stressing technique for composite laminates inspection by optical method. *Exp Tech* 1989;13:17–20.
- [156] Pieczonka L, Aymerich F, Staszewski WJ. Impact damage detection in light composite sandwich panels. *Procedia Eng* 2014;88:216–21.
- [157] Groves RM, James SW, Tatam RP. Full surface strain measurement using shearography. *Opt. Diagnostics Fluids, Solids, Combust.*, vol. 4448, International Society for Optics and Photonics; 2001, p. 142–52.
- [158] Groves RM, Chehura E, Li W, Staines SE, James SW, Tatam RP. Surface strain measurement: a comparison of speckle shearing interferometry and optical fibre Bragg gratings with resistance foil strain gauges. *Meas Sci Technol* 2007;18:1175–84.
- [159] Tay CJ, Toh SL, Shang HM, Lin QY. Direct determination of second-order derivatives in plate bending using multiple-exposure shearography. *Opt Laser Technol* 1994;26:91–8.
- [160] Mohan NK. The influence of multiple-exposure recording on curvature pattern using multi-aperture speckle shear interferometry. *Opt Commun* 2000;186:259–63.
- [161] Wang K, Tieu AK, Li E. Influence of displacement and its first- and second-order derivative components on curvature fringe formations in speckle shearography. *Appl Opt* 2002;41:4557–61.
- [162] Tay CJ, Fu Y. Determination of curvature and twist by digital shearography and wavelet transforms. *Opt Lett* 2005;30:2873–5. doi:10.1364/OL.30.002873.
- [163] Hung YY. Applications of digital shearography for testing of composite structures. *Compos Part B Eng* 1999;30:765–73.
- [164] Pechersky MJ. Determination of residual stresses by thermal relaxation and speckle correlation interferometry. *Strain* 2002;38:141–9.
- [165] Parlevliet PP, Bersee HEN, Beukers A. Residual stresses in thermoplastic composites—A study of the literature—Part II: Experimental techniques. *Compos Part A Appl Sci Manuf* 2007;38:651–65.
- [166] Lee J-R, Molimard J, Vautrin A, Surrel Y. Application of grating shearography and speckle shearography to mechanical analysis of composite material. *Compos Part A Appl Sci Manuf* 2004;35:965–76.
- [167] Lee J-R, Yoon D-J, Kim J-S, Vautrin A. Investigation of shear distance in Michelson interferometer-based shearography for mechanical characterization. *Meas Sci Technol* 2008;19:115303.
- [168] Shang HM, Hung YY, Luo WD, Chen F. Surface profiling using shearography. *Opt Eng*



- 2000;39:23–31.
- [169] Sim CW, Chau FS, Toh SL. Vibration analysis and non-destructive testing with real-time shearography. *Opt Laser Technol* 1995;27:45–9.
- [170] Valera JDR, Jones JDC. Vibration analysis by modulated time-averaged speckle shearing interferometry. *Meas Sci Technol* 1995;6:965–70.
- [171] Huang J-R, Ford HD, Tatam RP. Heterodyning of speckle shearing interferometers by laser diode wavelength modulation. *Meas Sci Technol* 1996;7:1721.
- [172] Kadlec M, Růžek R. A Comparison of Laser Shearography and C-Scan for Assessing a Glass/Epoxy Laminate Impact Damage. *Appl Compos Mater* 2012;19:393–407.
- [173] Ibrahim JS, Petzing JN, Tyrer JR. Deformation analysis of aircraft wheels using a speckle shearing interferometer. *Proc Inst Mech Eng Part G J Aersp Eng* 2004;218:287–95.
- [174] Bisle WJ, Scherling D, Kalms MK, Osten W. Improved shearography for use on optical non cooperating surfaces under daylight conditions. *AIP Conf Proc* 2001;557:1928–35.
- [175] Vollen MW, Vikhagen E, Wang G, Jensen AE, Haugland SJ. Application of shearography techniques for vibration characterization and damage detection in sandwich structures. *Optonor As Trondheim (Norway)*; 2005.
- [176] Pickering SG, Almond DP. Comparison of the defect detection capabilities of flash thermography and vibration excitation shearography. *Insight-Non-Destructive Test Cond Monit* 2010;52:78–81.
- [177] Ochôa P, Infante V, Silva JM, Groves RM. Detection of multiple low-energy impact damage in composite plates using Lamb wave techniques. *Compos Part B Eng* 2015;80:291–8.
- [178] Francis D, Tatam RP, Groves RM. Shearography technology and applications: a review. *Meas Sci Technol* 2010;21:102001.
- [179] Tyson IIIJ, Newman JW. Apparatus and method for performing electronic shearography. US5094528A, 1992.
- [180] Huang YH, Ng SP, Liu L, Li CL, Chen YS, Hung YY. NDT&E using shearography with impulsive thermal stressing and clustering phase extraction. *Opt Lasers Eng* 2009;47:774–81.
- [181] Liu Z, Gao J, Xie H, Wallace P. NDT capability of digital shearography for different materials. *Opt Lasers Eng* 2011;49:1462–9.
- [182] Abou-Khousa MA, Ryley A, Kharkovsky S, Zoughi R, Daniels D, Kreitinger N, et al. Comparison of X-Ray, millimeter wave, shearography and through-transmission



- ultrasonic methods for inspection of honeycomb composites. *AIP Conf Proc* 2007;894:999–1006.
- [183] Nyongesa HO, Otieno AW, Rosin PL. Neural fuzzy analysis of delaminated composites from shearography imaging. *Compos Struct* 2001;54:313–8.
- [184] Hung YY. Shearography and applications in experimental mechanics. *Proc. SPIE*, vol. 2921, 1997, p. 1–28.
- [185] Xie X, Zhou Z. Shearographic nondestructive testing for high-pressure composite tubes. *SAE Int* 2018;01:1219.
- [186] Macedo FJ, Benedet ME, Fantin AV, Willemann DP, da Silva FAA, Albertazzi A. Inspection of defects of composite materials in inner cylindrical surfaces using endoscopic shearography. *Opt Lasers Eng* 2018;104:100–8.
- [187] ASTM International. Standard practice for shearography of polymer matrix composites and sandwich core materials in aerospace applications - E2581 2014:1–10.
- [188] Newman JW. Method and apparatus for contrast enhanced photography of wind turbine blades. US20160063350A1, 2019.
- [189] Steinchen W, Yang L, Kupfer G, Mäckel P. Non-destructive testing of aerospace composite materials using digital shearography. *Proc Inst Mech Eng Part G J Aerosp Eng* 1998;212:21–30.
- [190] Pezzoni R, Krupka R. Laser-shearography for non-destructive testing of large-area composite helicopter structures. *Insight-Wigst THEN NORTHAMPTON-* 2001;43:244–8.
- [191] Yusof MY, Loganathan TM, Burhan I, Abdullah WSW, Mohamed MNI, Abidin IMZ, et al. Shearography technique on inspection of advanced aircraft composite material. *IOP Conf Ser Mater Sci Eng* 2019;554:12009.
- [192] Pagliarulo V, Farroni F, Ferraro P, Lanzotti A, Martorelli M, Memmolo P, et al. Combining ESPI with laser scanning for 3D characterization of racing tyres sections. *Opt Lasers Eng* 2018;104:71–7.
- [193] Peters WH, Ranson WF. Digital imaging techniques in experimental stress analysis. *Opt Eng* 1982;21:427–31.
- [194] McCormick N, Lord J. Digital image correlation. *Mater Today* 2010;13:52–4.
- [195] MESOCOS MS& CS. DIC measurement in engineering applications 2015:1–13. <http://image-correlation.com/assets/files/MESOCOS-DIC.pdf>.
- [196] Dong YL, Pan B. A review of speckle pattern fabrication and assessment for digital image correlation. *Exp Mech* 2017;57:1161–81.



- [197] Pan B. Digital image correlation for surface deformation measurement: historical developments, recent advances and future goals. *Meas Sci Technol* 2018;29:82001.
- [198] Hild F, Bouterf A, Roux S. Damage measurements via DIC. *Int J Fract* 2015;191:77–105.
- [199] Aparna ML, Chaitanya G, Srinivas K, Rao JA. Fatigue Testing of Continuous GFRP Composites Using Digital Image Correlation (DIC) Technique a Review. *Mater Today Proc* 2015;2:3125–31.
- [200] Caminero MA, Lopez-Pedrosa M, Pinna C, Soutis C. Damage assessment of composite structures using digital image correlation. *Appl Compos Mater* 2014;21:91–106.
- [201] Willems A, Lomov S V, Verpoest I, Vandepitte D. Drape-ability characterization of textile composite reinforcements using digital image correlation. *Opt Lasers Eng* 2009;47:343–51.
- [202] Elhajjar RF, Shams SS. A new method for limit point determination in composite materials containing defects using image correlation. *Compos Sci Technol* 2016;122:140–8.
- [203] Catalanotti G, Camanho PP, Xavier J, Dávila CG, Marques AT. Measurement of resistance curves in the longitudinal failure of composites using digital image correlation. *Compos Sci Technol* 2010;70:1986–93.
- [204] Dias GF, de Moura MFSF, Chousal JAG, Xavier J. Cohesive laws of composite bonded joints under mode I loading. *Compos Struct* 2013;106:646–52.
- [205] Furtado C, Arteiro A, Catalanotti G, Xavier J, Camanho PP. Selective ply-level hybridisation for improved notched response of composite laminates. *Compos Struct* 2016;145:1–14.
- [206] Smyl D, Antin K-N, Liu D, Bossuyt S. Coupled digital image correlation and quasi-static elasticity imaging of inhomogeneous orthotropic composite structures. *Inverse Probl* 2018;34:124005.
- [207] Sarasini F, Tirillò J, D’Altilia S, Valente T, Santulli C, Touchard F, et al. Damage tolerance of carbon/flax hybrid composites subjected to low velocity impact. *Compos Part B Eng* 2016;91:144–53.
- [208] Wang Y, Lava P, Coppieters S, De Strycker M, Van Houtte P, Debruyne D. Investigation of the uncertainty of DIC under heterogeneous strain states with numerical tests. *Strain* 2012;48:453–62.
- [209] Hedayati N, Hashemi R. Some practical aspects of digital image correlation technique to evaluate anisotropy coefficient and its comparison with traditional method. *J Test*



Eval 2019;48:1–17.

- [210] Liu Y, Nelson J, Holzner C, Andrews JC, Pianetta P. Recent advances in synchrotron-based hard x-ray phase contrast imaging. *J Phys D Appl Phys* 2013;46:494001.
- [211] Momose A. Recent advances in X-ray phase imaging. *Jpn J Appl Phys* 2005;44:6355–67.
- [212] Banhart J, Borbély A, Dzieciol K, Garcia-Moreno F, Manke I, Kardjilov N, et al. X-ray and neutron imaging – Complementary techniques for materials science and engineering. *Int J Mater Res* 2010;101:1069–79.
- [213] Fitzpatrick ME, Lodini A. Analysis of residual stress by diffraction using neutron and synchrotron radiation. CRC Press; 2003.
- [214] Zhou X-L, Chen S-H. Theoretical foundation of X-ray and neutron reflectometry. *Phys Rep* 1995;257:223–348.
- [215] Allen AJ, Hutchings MT, Windsor CG, Andreani C. Neutron diffraction methods for the study of residual stress fields. *Adv Phys* 1985;34:445–73.
- [216] Hutchings MT, Withers PJ, Holden TM, Lorentzen T. Introduction to the characterization of residual stress by neutron diffraction. CRC press; 2005.
- [217] Wang B. Viscoelastically prestressed composites: towards process optimisation and application to morphing structures. University of Hull, 2016.
- [218] Garcea SC, Wang Y, Withers PJ. X-ray computed tomography of polymer composites. *Compos Sci Technol* 2018;156:305–19.
- [219] Caballero L, Colomer FA, Bellot AC, Domingo-Pardo C, Nieto JLL, Ros JA, et al. Gamma-ray imaging system for real-time measurements in nuclear waste characterisation. *J Instrum* 2018;13:P03016–P03016.
- [220] Garcea SC, Sinclair I, Spearing SM, Withers PJ. Mapping fibre failure in situ in carbon fibre reinforced polymers by fast synchrotron X-ray computed tomography. *Compos Sci Technol* 2017;149:81–9.
- [221] Wang B, Tan D, Lee TL, Khong JC, Wang F, Eskin D, et al. Ultrafast synchrotron X-ray imaging studies of microstructure fragmentation in solidification under ultrasound. *Acta Mater* 2018;144:505–15.
- [222] Tavares PF, Leemann SC, Sjöström M, Andersson Å. The MAXIV storage ring project. *J Synchrotron Radiat* 2014;21:862–77.
- [223] Gruner SM. Study for a proposed Phase I Energy Recovery Linac (ERL) synchrotron light source at Cornell University. Thomas Jefferson National Accelerator Facility, Newport News, VA (US); 2001.



- [224] Cool TA, McIlroy A, Qi F, Westmoreland PR, Poisson L, Peterka DS, et al. Photoionization mass spectrometer for studies of flame chemistry with a synchrotron light source. *Rev Sci Instrum* 2005;76:94102.
- [225] Bilderback DH, Elleaume P, Weckert E. Review of third and next generation synchrotron light sources. *J Phys B At Mol Opt Phys* 2005;38:S773–97.
- [226] Di Cicco A, Aquilanti G, Minicucci M, Principi E, Novello N, Cognigni A, et al. Novel XAFS capabilities at ELETTRA synchrotron light source. *J. Phys. Conf. Ser.*, vol. 190, IOP Publishing; 2009, p. 12043.
- [227] Jiang M, Yang X, Xu H, Zhao Z, Ding H. Shanghai synchrotron radiation facility. *Chinese Sci Bull* 2009;54:4171.
- [228] Eriksson M, Ahlbäck J, Andersson Å, Johansson M, Kumbaro D, Leemann SC, et al. The MAX IV synchrotron light source. *Proc. IPAC2011, San Sebastián: Citeseer*; 2011, p. 1–4.
- [229] Liu L, Milas N, Mukai AHC, Resende XR, de Sá FH. The SIRIUS project. *J Synchrotron Radiat* 2014;21:904–11.
- [230] Jiao Y, Xu G, Cui X-H, Duan Z, Guo Y-Y, He P, et al. The HEPS project. *J Synchrotron Radiat* 2018;25:1611–8.
- [231] Zhao Z. Synchrotron light sources. *Synchrotron Radiat Mater Sci* 2018:1–33.
- [232] ASTM International. Standard practice for radiographic examination using computed radiography (photostimulable luminescence method) - E2033 2017:1–13.
- [233] ASTM International. Standard practice for radiographic examination of flat panel composites and sandwich core materials used in aerospace applications - E2662 2015:1–6.
- [234] Chadwick J. Possible existence of a neutron. *Nature* 1932;129:312.
- [235] Baruchel J, Hodeau J-L, Lehmann MS, Regnard J-R, Schlenker C. Neutron and synchrotron radiation for condensed matter studies. Springer; 1993.
- [236] Santisteban JR, Daymond MR, James JA, Edwards L. ENGIN-X: a third-generation neutron strain scanner. *J Appl Crystallogr* 2006;39:812–25.
- [237] Wang B, Seffen KA, Guest SD, Lee T-L, Huang S, Luo S, et al. In-situ neutron diffraction study of micromechanical shear failure in an aerospace composite. *AIAA SciTech 2020 Forum*, 2020, p. 1–12.
- [238] Aksenov VL. Reactor neutron sources. *Proc. 5th EPS Int. Conf. Large Facil., World Scientific*; 1995, p. 273–91.
- [239] Richter D, Springer T. A twenty years forward look at neutron scattering facilities in the



- OECD countries and Russia. 1998.
- [240] Shinohara T, Kai T, Oikawa K, Segawa M, Harada M, Nakatani T, et al. Final design of the Energy-Resolved Neutron Imaging System “RADEN” at J-PARC. *J Phys Conf Ser* 2016;746:12007.
- [241] Minniti T, Watanabe K, Burca G, Pooley DE, Kockelmann W. Characterization of the new neutron imaging and materials science facility IMAT. *Nucl Instruments Methods Phys Res Sect A Accel Spectrometers, Detect Assoc Equip* 2018;888:184–95.
- [242] Vontobel P, Lehmann EH, Hassanein R, Frei G. Neutron tomography: Method and applications. *Phys B Condens Matter* 2006;385–386:475–80.
- [243] Kockelmann W, Zhang SY, Kelleher JF, Nightingale JB, Burca G, James JA. IMAT – A new imaging and diffraction instrument at ISIS. *Phys Procedia* 2013;43:100–10.
- [244] Kockelmann W, Minniti T, Pooley D, Burca G, Ramadhan R, Akeroyd F, et al. Time-of-Flight Neutron Imaging on IMAT@ISIS: A New User Facility for Materials Science. *J Imaging* 2018;4:47.
- [245] Woracek R, Santisteban J, Fedrigo A, Strobl M. Diffraction in neutron imaging—A review. *Nucl Instruments Methods Phys Res Sect A Accel Spectrometers, Detect Assoc Equip* 2018;878:141–58.
- [246] Strobl M, Manke I, Kardjilov N, Hilger A, Dawson M, Banhart J. Advances in neutron radiography and tomography. *J Phys D Appl Phys* 2009;42:243001.
- [247] Kardjilov N, Manke I, Woracek R, Hilger A, Banhart J. Advances in neutron imaging. *Mater Today* 2018;21:652–72.
- [248] Vavilov VP, Burleigh DD. Review of pulsed thermal NDT: Physical principles, theory and data processing. *NDT E Int* 2015;73:28–52.
- [249] Atsushi M, Wataru Y, Kazuhiro K, Junko K, Chiho M, Tsukasa I, et al. X-ray phase imaging: From synchrotron to hospital. *Philos Trans R Soc A Math Phys Eng Sci* 2014;372:20130023.
- [250] Pracht M, Swiderski W. Analysis of the possibility of non-destructive testing to detect defects in multi-layered composites reinforced fibers by optical IR thermography. *Compos Struct* 2019;213:204–8.
- [251] Stoik C, Bohn M, Blackshire J. Nondestructive evaluation of aircraft composites using reflective terahertz time domain spectroscopy. *NDT E Int* 2010;43:106–15.
- [252] Ye Y, Ma K, Zhou H, Arola D, Zhang D. An automated shearography system for cylindrical surface inspection. *Measurement* 2019;135:400–5.
- [253] Senck S, Scheerer M, Revol V, Plank B, Hanneschläger C, Gusenbauer C, et al.



- Microcrack characterization in loaded CFRP laminates using quantitative two- and three-dimensional X-ray dark-field imaging. *Compos Part A Appl Sci Manuf* 2018;115:206–14.
- [254] De Simone ME, Cuomo S, Ciampa F, Meo M, Nitschke S, Hornig A, et al. Acoustic emission localization in composites using the signal power method and embedded transducers. *Nondestruct. Charact. Monit. Adv. Mater. Aerospace, Civ. Infrastructure, Transp.* XIII, vol. 10971, International Society for Optics and Photonics; 2019, p. 1097110.
- [255] Ashir M, Nocke A, Bulavinov A, Pinchuk R, Cherif C. Sampling phased array technology for the detection of voids in carbon fiber-reinforced plastics. *J Text Inst* 2019;110:1703–9.
- [256] Podymova NB, Kalashnikov IE, Bolotova LK, Kobeleva LI. Laser-ultrasonic nondestructive evaluation of porosity in particulate reinforced metal-matrix composites. *Ultrasonics* 2019;99:105959.
- [257] Bendada A, Sfarra S, Genest M, Paoletti D, Rott S, Talmy E, et al. How to reveal subsurface defects in Kevlar® composite materials after an impact loading using infrared vision and optical NDT techniques? *Eng Fract Mech* 2013;108:195–208.
- [258] Yang F, Ye X, Qiu Z, Zhang B, Zhong P, Liang Z, et al. The effect of loading methods and parameters on defect detection in digital shearography. *Results Phys* 2017;7:3744–55.
- [259] Centea T, Hubert P. Measuring the impregnation of an out-of-autoclave prepreg by micro-CT. *Compos Sci Technol* 2011;71:593–9.
- [260] Alam MK, Khan MA, Lehmann EH, Vontobel P. Study of the water uptake and internal defects of jute-reinforced polymer composites with a digital neutron radiography technique. *J Appl Polym Sci* 2007;105:1958–63.
- [261] Kam E, Reyhancan IA, Biyik R. A portable fast neutron radiography system for non-destructive analysis of composite materials. *Nukleonika* 2019;64:97–101.
- [262] Saeedifar M, Fotouhi M, Ahmadi Najafabadi M, Hosseini Toudeshky H, Minak G. Prediction of quasi-static delamination onset and growth in laminated composites by acoustic emission. *Compos Part B Eng* 2016;85:113–22.
- [263] Laureti S, Khalid Rizwan M, Malekmohammadi H, Burrascano P, Natali M, Torre L, et al. Delamination detection in polymeric ablative materials using pulse-compression thermography and air-coupled ultrasound. *Sensors* 2019;19:2198.
- [264] Ryu C-H, Park S-H, Kim D-H, Jhang K-Y, Kim H-S. Nondestructive evaluation of



- hidden multi-delamination in a glass-fiber-reinforced plastic composite using terahertz spectroscopy. *Compos Struct* 2016;156:338–47.
- [265] Pagliarulo V, Papa I, Lopresto V, Langella A, Ferraro P. Impact damage investigation on glass fiber-reinforced plate laminates at room and lower temperatures through ultrasound testing and electronic speckle pattern interferometry. *J Mater Eng Perform* 2019;28:3301–8.
- [266] Szebényi G, Hliva V. Detection of delamination in polymer composites by digital image correlation-experimental test. *Polymers (Basel)* 2019;11:523.
- [267] Ellison A, Kim H. Shadowed delamination area estimation in ultrasonic C-scans of impacted composites validated by X-ray CT. *J Compos Mater* 2019;0:1–13.
- [268] Yi Q, Tian GY, Malekmohammadi H, Zhu J, Laureti S, Ricci M. New features for delamination depth evaluation in carbon fiber reinforced plastic materials using eddy current pulse-compression thermography. *NDT E Int* 2019;102:264–73.
- [269] Li H, Zhou Z. Detection and characterization of debonding defects in aeronautical honeycomb sandwich composites using noncontact air-coupled ultrasonic testing technique. *Appl Sci* 2019;9:283.
- [270] Yi Q, Tian GY, Yilmaz B, Malekmohammadi H, Laureti S, Ricci M, et al. Evaluation of debonding in CFRP-epoxy adhesive single-lap joints using eddy current pulse-compression thermography. *Compos Part B Eng* 2019;178:107461.
- [271] Dai B, Wang P, Wang T-Y, You C-W, Yang Z-G, Wang K-J, et al. Improved terahertz nondestructive detection of debonds locating in layered structures based on wavelet transform. *Compos Struct* 2017;168:562–8.
- [272] Wen Y, Zhang S, Zhang Y. Detection and Characterization Method for Interface Bonding Defects of New Composite Materials. *IEEE Access* 2019;7:134330–7.
- [273] Fernandes H, Zhang H, Ibarra-Castanedo C, Maldague X. Fiber orientation assessment on randomly-oriented strand composites by means of infrared thermography. *Compos Sci Technol* 2015;121:25–33.
- [274] Mendoza A, Schneider J, Parra E, Obert E, Roux S. Differentiating 3D textile composites: A novel field of application for Digital Volume Correlation. *Compos Struct* 2019;208:735–43.
- [275] Prade F, Schaff F, Senck S, Meyer P, Mohr J, Kastner J, et al. Nondestructive characterization of fiber orientation in short fiber reinforced polymer composites with X-ray vector radiography. *NDT E Int* 2017;86:65–72.
- [276] Evans LM, Minniti T, Barrett T, Müller A von, Margetts L. Virtual qualification of novel



- heat exchanger components with the image-based finite element method. Proc. 9th Conf. Ind. Comput. Tomogr. (iCT), Padova, Italy, 2019.
- [277] Dornfeld D. Application of acoustic emission techniques in manufacturing. *NDT E Int* 1992;25:259–69.
- [278] Liu PF, Chu JK, Liu YL, Zheng JY. A study on the failure mechanisms of carbon fiber/epoxy composite laminates using acoustic emission. *Mater Des* 2012;37:228–35.
- [279] Lee WJ, Seo BH, Hong SC, Won MS, Lee JR. Real world application of angular scan pulse-echo ultrasonic propagation imager for damage tolerance evaluation of full-scale composite fuselage. *Struct Heal Monit* 2019;18:1943–52.
- [280] Garcia Perez P, Bouvet C, Chettah A, Dau F, Ballere L, Pérès P. Effect of unstable crack growth on mode II interlaminar fracture toughness of a thermoplastic PEEK composite. *Eng Fract Mech* 2019;205:486–97.
- [281] Hong S, Liu P, Zhang J, Xing F, Dong B. Visual & quantitative identification of cracking in mortar subjected to loads using X-ray computed tomography method. *Cem Concr Compos* 2019;100:15–24.
- [282] Zhang P, Wang P, Hou D, Liu Z, Haist M, Zhao T. Application of neutron radiography in observing and quantifying the time-dependent moisture distributions in multi-cracked cement-based composites. *Cem Concr Compos* 2017;78:13–20.
- [283] Safai M, Wang X. Synchronized Phased Array and Infrared Detector System for Moisture Detection. US20190113449A1, 2019.
- [284] Federici JF. Review of moisture and liquid detection and mapping using terahertz imaging. *J Infrared, Millimeter, Terahertz Waves* 2012;33:97–126.
- [285] de Parscau du Plessix B, Lefébure P, Boyard N, Corre S Le, Lefèvre N, Jacquemin F, et al. In situ real-time 3D observation of porosity growth during composite part curing by ultra-fast synchrotron X-ray microtomography. *J Compos Mater* 2019;53:4105–16.
- [286] Alam MK, Khan MA, Lehmann EH. Comparative study of water absorption behavior in biopol® and jute-reinforced biopol® composite using neutron radiography technique. *J Reinf Plast Compos* 2006;25:1179–87.
- [287] Oromiehie E, Garbe U, Gangadhara Prusty B. Porosity analysis of carbon fibre-reinforced polymer laminates manufactured using automated fibre placement. *J Compos Mater* 2019;0:1–15.
- [288] Wang S, Tran T, Xiang L, Liu Y. Non-destructive evaluation of composite and metallic structures using photo-acoustic Method. *AIAA Scitech 2019 Forum*, 2019, p. 2042.
- [289] Destic F, Bouvet C. Impact damages detection on composite materials by THz imaging.



- Case Stud Nondestruct Test Eval 2016;6:53–62.
- [290] Ranatunga V, Crampton SM, Jegley DC. Impact Damage Tolerance of Composite Laminates with Through-the-Thickness Stitches. AIAA Scitech 2019 Forum, 2019, p. 1045.
- [291] Aslan M. Investigation of damage mechanism of flax fibre LPET commingled composites by acoustic emission. *Compos Part B Eng* 2013;54:289–97.
- [292] Siriruk A, Woracek R, Pupilampu SB, Penumadu D. Damage evolution in VARTM-based carbon fiber vinyl ester marine composites and sea water effects. *J Sandw Struct Mater* 2019;21:2057–76.
- [293] Yuan Y, Wang S. Measurement of the energy release rate of compressive failure in composites by combining infrared thermography and digital image correlation. *Compos Part A Appl Sci Manuf* 2019;122:59–66.
- [294] Djabali A, Toubal L, Zitoune R, Rechak S. Fatigue damage evolution in thick composite laminates: Combination of X-ray tomography, acoustic emission and digital image correlation. *Compos Sci Technol* 2019;183:107815.
- [295] Lopato P, Chady T. Terahertz examination of fatigue loaded composite materials. *Int J Appl Electromagn Mech* 2014;45:613–9.
- [296] Dia A, Dieng L, Gaillet L, Gning PB. Damage detection of a hybrid composite laminate aluminum/glass under quasi-static and fatigue loadings by acoustic emission technique. *Heliyon* 2019;5:e01414.
- [297] Wagner P, Schwarzhaupt O, May M. In-situ X-ray computed tomography of composites subjected to fatigue loading. *Mater Lett* 2019;236:128–30.
- [298] Reid A, Marshall M, Kabra S, Minniti T, Kockelmann W, Connolley T, et al. Application of neutron imaging to detect and quantify fatigue cracking. *Int J Mech Sci* 2019;159:182–94.
- [299] Aggelis DG, Barkoula N-M, Matikas TE, Paipetis AS. Acoustic structural health monitoring of composite materials : Damage identification and evaluation in cross ply laminates using acoustic emission and ultrasonics. *Compos Sci Technol* 2012;72:1127–33.
- [300] Sfarra S, Regi M, Santulli C, Sarasini F, Tirillò J, Perilli S. An innovative nondestructive perspective for the prediction of the effect of environmental aging on impacted composite materials. *Int J Eng Sci* 2016;102:55–76.
- [301] Rahani EK, Kundu T, Wu Z, Xin H. Mechanical damage detection in polymer tiles by THz radiation. *IEEE Sens J* 2011;11:1720–5.



- [302] Arora H, Hooper PA, Dear JP. Dynamic response of full-scale sandwich composite structures subject to air-blast loading. *Compos Part A Appl Sci Manuf* 2011;42:1651–62.
- [303] Anisimov AG, Groves RM. EXTREME shearography: high-speed shearography instrument for in-plane surface strain measurements during an impact event. *Proc. SPIE*, vol. 11056, 2019, p. 1–8.
- [304] Sui T, Salvati E, Zhang H, Nyaza K, Senatov FS, Salimon AI, et al. Probing the complex thermo-mechanical properties of a 3D-printed polylactide-hydroxyapatite composite using in situ synchrotron X-ray scattering. *J Adv Res* 2019;16:113–22.
- [305] Stoik CD, Bohn MJ, Blackshire JL. Nondestructive evaluation of aircraft composites using transmissive terahertz time domain spectroscopy. *Opt Express* 2008;16:17039–51.
- [306] Jiang N, Yu T, Li Y, Pirzada TJ, Marrow TJ. Hygrothermal aging and structural damage of a jute/poly (lactic acid) (PLA) composite observed by X-ray tomography. *Compos Sci Technol* 2019;173:15–23.
- [307] Chelliah SK, Parameswaran P, Ramasamy S, Vellayaraj A, Subramanian S. Optimization of acoustic emission parameters to discriminate failure modes in glass–epoxy composite laminates using pattern recognition. *Struct Heal Monit* 2018;18:1253–67.
- [308] Mahmod MF, Bakar EA, Ramzi R, Harimon MA, Abdul Latif N, Mustapa MS, et al. Artificial neural network application for damages classification in fibreglass pre-impregnated laminated composites (FGLC) from ultrasonic signal. In: Zawawi MAM, Teoh SS, Abdullah NB, Mohd Sazali MIS, editors. *10th Int. Conf. Robot. Vision, Signal Process. Power Appl.*, Singapore: Springer Singapore; 2019, p. 567–73.
- [309] Saeed N, King N, Said Z, Omar MA. Automatic defects detection in CFRP thermograms, using convolutional neural networks and transfer learning. *Infrared Phys Technol* 2019;102:103048.
- [310] Hu C, Duan Y, Liu S, Yan Y, Tao N, Osman A, et al. LSTM-RNN-based defect classification in honeycomb structures using infrared thermography. *Infrared Phys Technol* 2019;102:103032.
- [311] Tu W, Zhong S, Shen Y, Incecik A, Fu X. Neural network-based hybrid signal processing approach for resolving thin marine protective coating by terahertz pulsed imaging. *Ocean Eng* 2019;173:58–67.

